



รายงานวิจัยฉบับสมบูรณ์

โครงการ

ความสัมพันธ์ระหว่างการจัดเรียงตัวของใยโครมาตินและความสามารถ ในการเจริญพันธุ์ในเซลล์อสุจิของมนุษย์

The relationship between the packaging of chromatin and reproductive capacity in human spermatozoa

โดย

ดร. ศิริกุล มะโนจันทร์

รายงานวิจัยฉบับสมบูรณ์

โครงการ

ความสัมพันธ์ระหว่างการจัดเรียงตัวของใยโครมาตินและความสามารถ ในการเจริญพันธุ์ในเซลล์อสุจิของมนุษย์ The relationship between the packaging of chromatin and reproductive capacity in human spermatozoa

ผู้วิจัย

ดร. ศิริกุล มะโนจันทร์ สาขาเซลล์วิทยา สถานวิทยาศาสตร์พรีคลินิก คณะแพทยศาสตร์ มหาวิทยาลัยธรรมศาสตร์

สนับสนุนโดยสำนักงานกองทุนสนับสนุนการวิจัย (สกว.) และสำนักงาน คณะกรรมการการอุดมศึกษา (สกอ.)

(ความเห็นในรายงานนี้เป็นของผู้วิจัย สกอ. และ สกว. ไม่จำเป็นต้องเห็นด้วยเสมอไป)

Acknowledgements

The study entitled "The relationship between the packaging of chromatin and

reproductive capacity in human spermatozoa" was supported by grant from Thailand

Research Fund and Commission on Higher Education (Grant No. MRG4980207).

I would like to express my deep gratitude and my faithfulness to my mentor, Professor

Dr. Prasert Sobhon, Department of Anatomy, Faculty of Science, Mahidol University for

his esteemed supervisory, guidance, criticism and encouragement throughout the

course of this project.

I would like to extend my gratefulness to Professor Dr. Kovit Pattanapanyasat and Miss

Kasama Sukapirom, Division of Instruments for Research, Office for Research and

Development, Mahidol University for their valuable help in assessment of DNA damage

using Flow Cytometry.

I very appreciate the kindness of Assistant Professor Charoenchai Chiamchanya,

Division of Obstetrics and Gynecology, Faculty of Medicine, Thammasat University and

Miss Jirattikan Chaiya, Infertility Clinic, Thammasat University Hospital, Thammasat

University for their assistant in semen analysis.

Finally, I would like to thank to all volunteers, who donated their semen for this

research.

Sirikul Manochantr

Thammasat University

2008

Abstract

Project Code: MRG4980207

Project Title: The relationship between the packaging of chromatin and reproductive

capacity in human spermatozoa

Investigator: Sirikul Manochantr

Division of Cell Biology, Department of Preclinical Science, Faculty of

Medicine, Thammasat University

E-mail Address: bsirikul@yahoo.com

Project Period: July 1st 2006 – June 30th 2008

The various spermatozoa types present in an ejaculate differ in their motility and morphology. However, little is known about nuclear maturity of these spermatozoa and their relationship with morphological and motile characteristics. Histone-to-protamine exchange is a late spermiogenesis event, along with acrosome formation, membrane remodeling and other significant morphological and biochemical events those are necessary for normal sperm function. Therefore, protamines are considered as a good marker of sperm nuclear maturity. The aim of the present study is to investigate the relationship between DNA/chromatin integrity and sperm quality as measured by conventional semen parameters. The study group consisted of 49 patients attending the Center for Assisted Reproduction and Embryology, Thammasat University Hospital, Thailand for diagnostic semen analysis. Semen analysis was carried out to assess sperm concentration, motility, and morphology. The remaining aliquot of each semen sample was processed for the study of chromatin condensation and DNA integrity using transmission electron microscopy, chromomysin A3 (CMA3) assay and TUNNEL assay. Following the semen analysis, 49 patients were divided into 4 groups according to the percentage of morphologically normal spermatozoa, >30%; 14-30%; 4-14% and <4% normal morphology. The ultrastructural analysis showed heterogeneity in sperm nuclear morphology with some spermatozoa showing the round nucleus and other spermatozoa showing a more elongated nucleus. The disruption in chromatin condensation, identified by a coarse granular pattern and contains numerous vacuoles, in the spermatozoa from infertile couples is observed. Immunoreactivity with anti-TP was increased in spermatozoa of patients with morphologically normal spermatozoa <4%, while staining with anti-protamine antibodies was increased in spermatozoa of patients with morphologically normal spermatozoa >4%. This finding indicating the maturation defect as TP are retained in the spermatozoa of infertile couples. The relationship of the incidence of spermatozoa with abnormal chromatin condensation and parameters of basic semen analysis was investigated. The sperm concentrations were gradually reduced in patients with lower percentage of morphologically normal spermatozoa 14-30% (149.84±16.58 M/ml), 4-14% (125.54±11.59 M/ml), <4% (78.81±16.09 M/ml), versus patients with morphologically normal spermatozoa >30% (179.88±29.30 M/ml; P<0.05). Significantly lower percentages of sperm motility were recorded between the 4 different morphological groups, namely 57.8%±6.12, 48.5%±4.78, 43.24%±3.49 and 25.78%±6.76, respectively (P< 0.05). Spearman's correlation analysis indicated that the percentage of morphologically normal spermatozoa as recorded by strict criteria was significantly correlated with the concentration (r = 0.45, P = 0.001) and motility (r = 0.36, P = 0.01). The inversely correlations were found between the percentage of protamine deficiency spermatozoa (CMA3 positive) and concentration (r = -0.33, P = 0.009), motility (r = -0.53, P = 0.00) and normal morphology (r = -0.41, P = 0.002) while the other seminal parameters were less well correlated. Linear regression analysis revealed that the percentage of DNA damage spermatozoa were negatively correlated with concentration (r = -0.31, P = 0.01), motility (r = -0.46, P = 0.00) and normal morphology (r = -0.29, P = 0.02). In addition, patients with morphologically normal spermatozoa <4% have the significantly higher percentages of CMA3 and TUNNEL positive spermatozoa whereas the significantly lower percentage of sperm motility. The relationship between the percentages of CMA3 and TUNNEL positive spermatozoa also showed a significantly positive correlation with each other (r = 0.68, P = 0.00). These finding indicated that patients with abnormal semen parameters (decreased concentration, low motility, abnormal morphology) carrying higher loads of DNA-damaged spermatozoa, therefore seeking ART is of concern. The classical semen parameters do not give directly information about chromatin condensation and DNA integrity therefore additional strategies might be required to further improve the characterization of the semen quality.

Key words: male infertility, chromatin condensation, protamine deficiency, DNA integrity

บทคัดย่อ

รหัสโครงการ: MRG4980207

ชื่อโครงการ: ความสัมพันธ์ระหว่างการจัดเรียงตัวของใยโครมาตินและความสามารถในการ

เจริญพันธุ์ ในเซลล์อสุจิของมนุษย์

ชื่อนักวิจัย: ศิริกุล มะโนจันทร์

สาขาเซลล์วิทยา สถานวิทยาศาสตร์พรีคลินิก คณะแพทยศาสตร์

มหาวิทยาลัยธรรมศาสตร์

E-mail Address: bsirikul@yahoo.com

ระยะเวลาโครงการ: 1 กรกฎาคม 2549 – 30 มิถุนายน 2551

น้ำอสุจิประกอบด้วยอสุจิที่มีความแตกต่างกันทั้งทางด้านรูปร่างและการเคลื่อนที่ อย่างไรก็ตาม ข้อมูลเกี่ยวกับความสมบูรณ์ของนิวเคลียสของอสุจิเหล่านี้และความสัมพันธ์กับรูปร่างและการ เคลื่อนที่ยังไม่เป็นที่ทราบอย่างแน่ชัด ในระยะท้ายของการสร้างอสุจิจะมีการแทนที่โปรทีน histone ด้วย protamine พร้อมกับการสร้างอะโครโซม และการเปลี่ยนแปลงทางกายภาพและ ชีวเคมี ซึ่งส่งผลต่อการทำหน้าที่ของอสุจิ ดังนั้น protamine จึงเป็นตัวบ่งชี้ความสมบูรณ์ของ นิวเคลียสที่ดี เนื่องจาก protamine เป็นโปรทีนที่เข้าไปแทนที่ histone ในช่วงท้ายของการสร้าง อสุจิ การศึกษาในครั้งนี้มีวัตถุประสงค์เพื่อศึกษาความสัมพันธ์ระหว่างความสมบูรณ์ของโครมา ทิน/ดีเอ็นเอกับคุณภาพของอสุจิตามตัวบ่งชี้พื้นฐาน กลุ่มตัวอย่างประกอบด้วยผู้ป่วยที่เข้ารับ การรักษา ณ หน่วยผู้มีบุตรยาก รพ. ธรรมศาสตร์เฉลิมพระเกียรติ จำนวน 49 ราย น้ำอสุจิที่ได้ ถูกนำไปตรวจสอบตามวิธีมาตรฐานทางด้านจำนวนอสุจิ, การเคลื่อนที่ของอสุจิ, และรูปร่างของ อสุจิ น้ำอสุจิส่วนที่เหลือถูกนำไปศึกษาการขดของใยโครมาทินและความสมบูรณ์ของดีเอ็นเอ โดยกล้องจุลทรรศน์อิเลคตรอนแบบส่องผ่าน, การทดสอบด้วย CMA3 และ และการทดสอบ TUNNEL ภายหลังการตรวจวิเคราะห์น้ำอสุจิ ผู้ป่วยทั้ง 49 ราย ถูกแบ่งออกเป็น 4 กลุ่ม ตาม ร้อยละของอสุจิที่มีรูปร่างสมบูรณ์ ได้แก่ กลุ่มที่มีอสุจิที่มีรูปร่างสมบูรณ์ > 30%; 14-30%; 4-14% และ < 4% ตามลำดับ จากการศึกษาโครงสร้างแบบละเอียดพบว่า อสุจิจากคู่สมรสที่มีบุตร ยากมีรูปร่างหลายแบบทั้งที่มีนิวเคลียสกลมและนิวเคลียสยาวเรียว ภายในนิวเคลียสมีการขดตัว ของโครมาทินแบบกระจัดกระจายและมีช่องว่างภายในนิวเคลียสจำนวนมาก ผลการศึกษาการ กระจายตัวของโปรทีนในนิวเคลียส พบว่า อสุจิของคู่สมรสที่มีบุตรยาก มีการกระจายของ transition protein เพิ่มมากขึ้นในกลุ่มที่มีอสุจิที่มีรูปร่างสมบูรณ์น้อยกว่า 4% ในขณะที่การ กระจายของ protamine จะเพิ่มมากขึ้นในกลุ่มที่มีอสุจิที่มีรูปร่างสมบูรณ์มากกว่า 4% ข้อมูล ้ ดังกล่าวบ่งชี้ถึงความผิดปกติในด้านความสมบูรณ์ของการสร้างอสุจิ เมื่อศึกษาความสัมพันธ์

ระหว่างอุบัติการของอสุจิที่มีการขดตัวของใยโครมาทินที่ผิดปกติและตัวบ่งชี้พื้นฐานทางด้าน คุณภาพของอสุจิ พบว่า จำนวนอสุจิจะลดลงเป็นลำดับตามร้อยละของอสุจิที่มีรูปร่างสมบูรณ์, 14-30% (149.84±16.58 M/ml), 4-14% (125.54±11.59 M/ml), <4% (78.81±16.09 M/ml), เมื่อเปรียบเทียบกับกลุ่มที่มีอสุจิที่มีรูปร่างสมบูรณ์มากกว่า 30% (179.88±29.30 M/ml; P<0.05). นอกจากนี้ ยังพบการลดลงอย่างมีนัยสำคัญ (P<0.05) ของร้อยละของอสุจิที่เคลื่อนที่ ได้แก่ 57.8%±6.12, 48.5%±4.78, 43.24%±3.49 และ 25.78%±6.76 ตามลำดับ การวิเคราะห์ ความสัมพันธ์ด้วย Spearman พบว่า ร้อยละของอสุจิที่มีรูปร่างสมบูรณ์ มีความสัมพันธ์โดยตรง กับจำนวนอสุจิ (r = 0.45, P = 0.001) และการเคลื่อนที่ของอสุจิ (r = 0.36, P = 0.01).อย่างมี นัยสำคัญทางสถิติ นอกจากนี้ยังพบว่า ร้อยละของอสุจิที่มีภาวะขาด protamine มีความสัมพันธ์ ในเชิงลบอย่างมีนัยสำคัญทางสถิติกับจำนวนอสุจิ (r = -0.33, P = 0.009), การเคลื่อนที่ของอสุจิ (r = -0.53, P = 0.00) และจำนวนอสุจิที่มีรูปร่างสมบูรณ์ (r = -0.41, P = 0.002) การวิเคราะห์ พบว่า ร้อยละของอสุจิที่มีดีเอ็นเอฉีกขาด มี ความสัมพันธ์โดยใช้ linear regression ความสัมพันธ์ในเชิงลบกับจำนวนอสุจิ (r = -0.31, P = 0.01), การเคลื่อนที่ของอสุจิ (r = -0.46, P = 0.00) และจำนวนอสุจิที่มีรูปร่างสมบูรณ์ (r = -0.29, P= 0.02). นอกจากนี้ยังพบว่า ผู้ป่วยที่ มือสุจิที่มีรูปร่างสมบูรณ์น้อยกว่า 4% จะมือสุจิที่มีภาวะขาด protamine และมือสุจิที่มีดีเอ็นเอฉีก ขาดสูงขึ้น ในขณะที่มีร้อยละอสุจิที่มีการเคลื่อนที่ปกติลดลงอย่างมีนัยสำคัญทางสถิติ นอกจากนั้นยังพบว่าร้อยละของอสุจิที่มีภาวะขาด protamine มีความสัมพันธ์กับร้อยละของอสุจิ ์ ที่มีดีเอ็นเอฉีกขาดอย่างมีนัยสำคัญทางสถิติ (r = 0.68, P = 0.00) การศึกษาในครั้งนี้แสดงให้ เห็นว่า ผู้ป่วยที่มีอสุจิผิดปกติ (จำนวนอสุจิลดลง, การเคลื่อนที่ลดลง, รูปร่างผิดปกติ) จะมีร้อย ละของอสุจิที่มีดีเอ็นเอฉีกขาดสูงขึ้น ทำให้เกิดภาวะไม่เจริญพันธุ์ ดังนั้นจึงจำเป็นต้องอาศัย เทคโนโลยีช่วยการเจริญพันธุ์ นอกจากนี้การศึกษาในครั้งนี้ยังแสดงให้เห็นว่าการตรวจน้ำอสุจิ โดยวิธีพื้นฐานไม่ให้ข้อมูลที่เกี่ยวข้องกับการขดของโครมาทินและความสมบูรณ์ของดีเอ็นเอซึ่ง บ่งชี้ถึงการเจริญพันธุ์ของอสุจิ ดังนั้นอาจจำเป็นต้องเพิ่มยุทธวิธีบางอย่าง เพื่อให้การตรวจน้ำ อสุจิมีความแม่นยำมากขึ้น

คำสำคัญ ภาวะไม่เจริญพันธุ์เพศชาย, การขดของโครมาทิน, ภาวะขาดโปรทามีน, การฉีกขาด ของดีเอ็นเอ

Table of Contents

	Page
Abstract	i
Table of Contents	٧
List of Tables	vii
List of Figures	viii
Executive Summary	хi
Introduction	1
Literature Review	
Sperm Production: Spermatogenesis	3
Chromatin Organization during Spermatogenesis in Mammalian Male Germ Cells	5
Chromatin Organization in Somatic Cells	7
DNA Packaging in Mammalian Male Germ Cells	9
Human Male Infertility	13
Etiology of sperm DNA damage	13
Objectives	17
Materials and Methods	
Preparation of Semen Samples	18
Preparation of Human Spermatozoa for TEM	18
Electron Microscopy Study	18
Preparation of the Spermatozoa for Immunoelectron Microscopic Study	19

Table of Contents (Cont.)

		Page
	Immunogold Electron Microscopic Analysis	19
	Semen Analysis	20
	Evaluation of Sperm Morphology	20
	Chromomycin A3 (CMA3) Assay	20
	Terminal Deoxynucleotidyl Transferase Nick End Labeling (TUNNEL) Assay	21
	Statistical Analysis	21
Resu	Its	
	Ultrastructure of Spermatozoa from Infertile Couples	22
	Distribution of Transition Protein and Protamines in Spermatozoa of Infertile Couples as Studied by Immunoelectron Microscopy	26
	The Assessment of Human Ejaculated Spermatozoa	34
	Evaluation of Sperm Morphology	38
	CMA3 Assay for Protamine-Deficiency Spermatozoa	41
	Terminal Deoxynucleotidyl Transferase Nick End Labeling (TUNNEL) Assay	42
Discu	ussion	49
Conc	lusion	53
Biblio	ography	54
Outpo	ut	65
Appe	ndix	66

List of Tables

Та	ble	Page
1	Analysis of the standard semen parameter in difference sperm morphological groups.	35
2	Comparison of sperm morphology in difference sperm morphological groups.	38
3	CMA3 assay and TUNNEL assay in the spermatozoa from difference sperm morphological groups.	44
4	Correlation between the percentage of CMA3 positive spermatozoa and sperm concentration.	47
5	Correlation between the percentage of TUNNEL positive spermatozoa and sperm concentration.	47

List of Figures

Fig	jure	Page
1	Schematic of the levels of organization of chromatin and their folding into a chromosome.	8
2	DNA packing structures in somatic vs. sperm nuclei.	10
3	The process of chromatin reorganization in the spermatid.	11
4	TEM micrograph of longitudinal section of human spermatozoa	23
5	TEM micrographs of longitudinal and cross sections of immature spermatozoa characterized by round to oval nuclei	24
6	TEM micrographs of longitudinal and cross sections of immature spermatozoa characterized by nuclei with incomplete chromatin condensation	25
7	TEM micrographs of spermatozoa from infertile couples incubated in the absence of primary antibody and labeled with immunogold.	27
8	TEM micrographs of spermatozoa from infertile couples with morphologically normal spermatozoa > 4% stained with anti-protamine 1 antibody and labeled with immunogold.	28
9	TEM micrographs of spermatozoa from infertile couples with morphologically normal spermatozoa < 4% stained with anti-protamine 1 antibody and labeled with immunogold.	29
10	TEM micrographs of spermatozoa from infertile couples with morphologically normal spermatozoa > 4% stained with anti-protamine 2 antibody and labeled with immunogold.	30
11	TEM micrographs of spermatozoa from infertile couples with morphologically normal spermatozoa < 4% stained with anti-protamine 2 antibody and labeled with immunogold.	31

List of Figures (Cont.)

Fig	ure	Page
12	TEM micrographs of spermatozoa from infertile couples with morphologically normal spermatozoa > 4% stained with anti-transition protein antibody and labeled with immunogold.	32
13	TEM micrographs of spermatozoa from infertile couples with morphologically normal spermatozoa < 4% stained with anti-transition protein antibody and labeled with immunogold.	33
14	A comparison of concentration, motility, and progressive motility in patients divided according to morphologically characteristics.	36
15	Correlations between the percentage of morphologically normal spermatozoa and concentration, motility, and progressive motility.	37
16	A comparison of sperm morphology in difference sperm morphological groups.	39
17	Correlations between the percentage of morphologically normal spermatozoa and the percentages of head defect and cytoplasmic droplet.	40
18	Fluorescence micrograph of spermatozoa stained with CMA3.	41
19	Flow cytometry analysis of presence of DNA nicks occurs in the ejaculated spermatozoa.	43
20	A comparison of CMA3 positive spermatozoa and TUNNEL positive spermatozoa in difference sperm morphological groups.	44
21	Correlations between the percentage of CMA3 positive spermatozoa and concentration, the percentage of motility, and the percentage of normal morphology.	45
22	Correlations between the percentage of TUNNEL positive spermatozoa and concentration, the percentage of motility, and the percentage of normal morphology.	46

List of Figures (Cont.)

Figure	Page
23 Correlations between the percentages of TUNNEL positive spermatozoa	48
and CMA3 positive spermatozoa.	

Executive Summary

Project Title: The relationship between the packaging of chromatin and reproductive capacity in human spermatozoa

Investigators:

1. Dr. sirikul Manochantr (Principle investigator)

Division of Cell Biology

Department of Preclinical Science

Faculty of Medicine

Thammasat University

2. Assist. Professor Charoenchai Chiamchanya

Division of Obstetrics and Gynecology,

Department of Clinical Science

Faculty of Medicine,

Thammasat University

3. Professor Dr. Prasert Sobhon (Mentor)

Department of Anatomy

Faculty of Science

Mahidol University

Introduction

Sperm chromatin is a highly compact and complex structure and is capable of decondensation–features that must be present in order for a spermatozoon to be considered fertile. Any form of sperm chromatin abnormalities or DNA damage may result in male infertility. DNA integrity in sperm is also essential for the accurate transmission of genetic information and, in turn, the maintenance of good health in future generations (1).

During spermatogenesis and spermiogenesis of vertebrates, the chromatin undergoes extensive molecular reorganization and condensation that renders it more compact and metabolically inert as all paternal genes are switched off, and the chromatin must be

contained within the highly reduced volume of the sperm nucleus (2, 3). Thus, the paternal genome is protected against physical damage and chemical mutagenesis during transport to the site of fertilization (4).

Dramatic biochemical and ultrastructural changes in nuclei occur as mammalian spermatids develop into mature spermatozoa. Histones of spherically shaped nuclei possessing fine granular chromatin are replaced by more basic proteins, the transition proteins, in elongating and condensing nuclei; and these basic nucleoproteins are then replaced by even more basic sperm-specific nucleoproteins, the protamines, in mature spermatids with compact chromatin (5-7).

It has been suggested that the functional status of ejaculated sperm nuclei could result from these complex structural and biochemical alterations. Thus, penetration through the oocyte vestments could be facilitated for elongated spermatozoa with dramatically condensed chromatin (4). Subsequently, the early stages of embryogenesis might depend on nuclear proteins and chromatin organization (8, 9).

This state of chromatin condensation may be altered by various factors, such as a shortage of zinc from the prostate (10), or alterations in protamines (11). Various reports in mammalian species support the hypothesis of a close relationship between nuclear maturity and fertility of ejaculated sperm (12-14).

The assessment of chromatin status is very important when evaluating the ability of spermatozoa to fertilize. Many techniques have been described for the evaluation of chromatin status, such as optical microscopy (15), electron microscopy (16, 17) and flow cytometry (18). Sperm chromatin defects have been correlated with the reduced ability of spermatozoa to fertilize both in the context of assisted reproduction techniques (19-21) and in the general population (22). Moreover, patients with fertility problems have often been characterized by an increased frequency of spermatozoa with abnormal chromatin (15, 23).

In this study, different groups of patients are examined, both fertile and infertile, in order to analyse the standard parameters of semen analysis and those that depend on the state of sperm chromatin. The ultrastructural charactics, nuclear shape and chromatin texture of human spermatozoa are analyzed through the use of transmission electron microscopy (TEM). Size, shape, and chromatin texture parameters were found to be

salient indicators of stage-related nuclear transformations from early spermiogenesis to the end of epididymal transit. Thus, it is possible to observe differences between patient groups. The protamines in the nucleus of both fertile and infertile spermatozoa were analyzed by using CMA3 assay. Furthermore, the distribution of transition protein and protamines in spermatozoa from fertile in infertile were observed to clarify whether it is related to reproductive capacity or not. The data obtain from this study might be serve as a diagnostic tool in clinical practice for IUI, IVF and ICSI treatments

Objectives

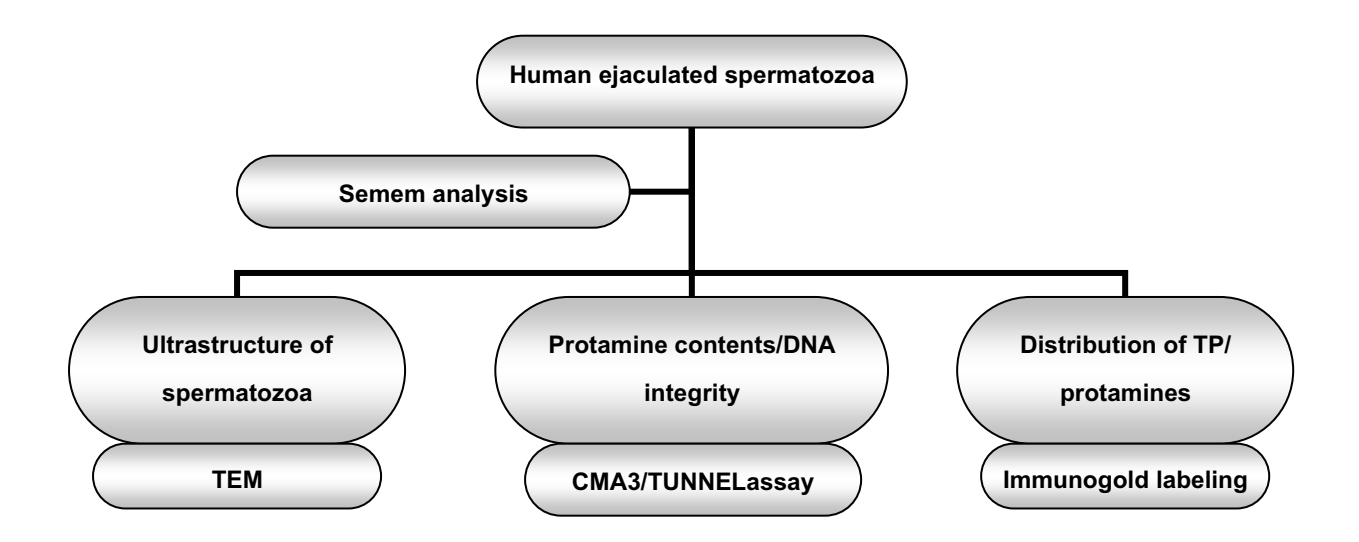
1. Overall objective

The overall objective of this research is to investigate the relationship between chromatin packaging, sperm quality and DNA integrity in spermatozoa from infertile couples.

2. Specific objectives

- 2.1 To study the ultrastructure of spermatozoa from infertile couples by transmission electron microscopy.
- 2.2 To study the chromatin packaging in the nucleus of spermatozoa from infertile couples by transmission electron microscopy.
- 2.3 To study the distribution of transition protein and protamines in the nucleus of spermatozoa from infertile couples.
- 2.4 To evaluate the protamine content in nucleus of spermatozoa from infertile couples.
- 2.5 To study the DNA integrity in the nucleus of spermatozoa from infertile couples.
- 2.6 To deduce the relationship between the pattern of chromatin organization, the basic nuclear protein profiles and the reproductive capacity.

Methodology



Results

1. Ultrastructure of Spermatozoa from Infertile Couples

The ultrastructural analysis showed heterogeneity in sperm nuclear morphology with some spermatozoa showing the round nucleus and other sperm showing a more elongated nucleus. The disruption in chromatin condensation, identified by a coarse granular pattern and contains numerous vacuoles, in the spermatozoa from infertile couples is observed. In addition, spermatozoa from infertile couples tend to have multiple defects involving: acrosomal disorders, cytoplasmic residues, lack of peripheral microtubules, additional axoneme and midpiece abnormalities. As far as immaturity is concerned, the nuclei were irregularly shaped, generally elliptical or spherical, with uncondensed chromatin and residual cytoplasmic droplets surrounding the nucleus or midpiece regions. Binucleated spermatozoa are generally observed. Axonemal structure is often altered, lacking central microtubule, and some doublets has incomplete or absent dynein arms. The tail is often rolled up into cytoplasmic droplets with a disorganized fibrous sheath and accessory fibers, mitochondrial helix is badly assembled.

2. Distribution of Transition Protein and Protamines in Spermatozoa of Infertile Couples as Studied by Immunoelectron Microscopy

Immunogold labeling with anti-protamine1 antibody was found over the nuclei of spermatozoa from infertile couples. The labeling was especially abundant in the area of highly condensed chromatin, with only occasional gold particles observed over the area of incomplete chromatin condensation. The labeling appeared to be directly proportional to its condensation state. There was no labeling in the nuclear vacuoles of the sperm nuclei. The cytoplasm showed only minimal background level of labeling. In control group, only a low background immunogold labeling can be observed.

Immunogold labeling with anti-protamine2 antibody revealed the distribution of gold particles over the nuclei of spermatozoa from infertile couples, and their abundance is directly proportional to the state of chromatin condensation. Only a few gold particles were found in the areas of incomplete condensed chromatin. Interestingly, higher amount of immunogold labeling was observed in the nuclei of spermatozoa from infertile couples with morphologically normal spermatozoa >4% in comparison to spermatozoa from infertile couples with morphologically normal spermatozoa <4%. There was an absence of labeling in the nuclear vacuoles of the sperm nuclei. No labeling was also obtained in the cytoplasm of the spermatozoa. In control group which was incubated in the absence of primary antibody, only background labeling was observed.

When the spermatozoa from infertile couples with morphologically normal spermatozoa >4% were incubated with anti-TP antibody, little to no labeling was observed over the nuclei. In contrast, the labeling was prominent over the granular and condensed chromatin of spermatozoa from infertile couples with morphologically normal spermatozoa <4%. Only background level of labeling can be observed in control group.

3. The Assessment of Human Ejaculated Spermatozoa

Aliquots from 49 ejaculates were assessed using the computer-assisted semen analyzer (CASA) and Makler counting chamber. Following the semen analysis, the 49 men were divided according to the percentage of normal sperm morphology into 4 groups, Group I: Normal morphology >30%; Group II: Normal morphology 14-30%; Group III: Normal morphology 4-14%; Group IV: Normal morphology <4%. The standard seminal

parameters (concentration, motility and progressive motility) showed significant difference between groups (Table 1). The concentrations were gradually reduced in infertile couples with morphologically normal spermatozoa 14-30% (149.84±16.58 x $10^6/\text{ml}$), 4-14% (125.54±11.59 x $10^6/\text{ml}$), <4% (78.81±16.09 x $10^6/\text{ml}$), versus infertile couples with morphologically normal spermatozoa >30% (179.88±29.30 x $10^6/\text{ml}$); P<0.05). Significantly lower percentages of sperm motility (mean±SEM) were recorded between the 4 different morphological groups, namely 57.8%±6.12, 48.5%±4.78, 43.24%±3.49 and 25.78%±6.76, respectively (P<0.05). Spearman's correlation analysis indicated that the percentage of morphologically normal spermatozoa is significantly correlated with the concentration (r = 0.45, P = 0.001). A positive correlation existed between percentage of normal morphology as recorded by strict criteria and sperm motility (r = 0.36, P = 0.01) and also progressive motility (r = 0.27).

Table 1 Analysis of the standard semen parameter in difference sperm morphological groups, >30%; 14-30%; 4-14% and <4% normal morphology.

	>30%	14-30%	4-14%	<4%
	Normal	Normal	Normal	Normal
	morphology	morphology	morphology	morphology
	(N=5)	(N=14)	(N=21)	(N=9)
Volume (ml)	3.04 ± 0.07	2.32 ± 0.21	2.58 ± 0.19	3.10 ± 0.26
Concentration (x10 ⁶ /ml)	179.88 ± 29.30	149.84 ± 16.58	125.54 ± 11.59	78.81 ± 16.09
Motility (% grade A+B)	57.8 ± 6.12	48.5 ± 4.78	43.24 ± 3.49	25.78 ± 6.76
PMC (%)	44.8 ± 4.93	35.67 ± 4.08	33.30 ± 0.23	21.22 ± 6.04
Morphology (% normal morphology)	36.4 ± 2.29	21.78 ± 1.36	7.76 ± 0.68	2.44 ± 0.60

Values represent the mean plus or minus the standard error of mean.

4. Evaluation of Sperm Morphology

An analysis of sperm morphology was carried out for the previously established groups (Table 2). The head defects were found as a majority of all defects in all groups. The percentage of head defects were negatively correlated to the percentage of normal morphology (r = -0.75, P = 0.00) while the other defects are less well correlated, excepted for the percentage of cytoplasmic droplets (r = -0.36, P = 0.006)

Table 2 Comparison of sperm morphology in difference sperm morphological groups, >30%; 14-30%; 4-14% and <4% normal morphology.

	>30%	14-30%	4-14%	<4%
	Normal	Normal	Normal	Normal
	morphology	morphology	morphology	morphology
	(N=5)	(N=14)	(N=21)	(N=9)
Normal morphology (%)	36.4 ± 2.29	21.78 ± 1.36	7.76 ± 0.68	2.44 ± 0.60
Head defects (%)	50 ± 3.59	65.86 ± 2.04	73.95 ± 1.81	76.22 ± 3.34
Neck defects (%)	5.00 ± 1.64	4.57 ± 1.16	6.14 ± 1.04	5.11 ± 1.76
Tail defects (%)	9.80 ± 3.01	5.57 ± 1.45	7.14 ± 1.00	10.11 ± 2.45
Cytoplasmic droplets (%)	0.60 ± 0.60	1.21 ± 0.54	2.33 ± 0.35	2.67 ± 1.00

Values represent the mean plus or minus the standard error of mean

5. CMA3 Assay

CMA3 assay for protamine-deficiency spermatozoa revealed a significantly higher percentage of CMA3 positive spermatozoa in Group II (morphologically normal spermatozoa 14-30%), Group III (morphologically normal spermatozoa 4-14%) and Group IV (morphologically normal spermatozoa <4%) compared to Group I (morphologically normal spermatozoa >30%; Table 3). An analysis was also performed on the relationship between the protamine contents and the standard seminal

parameters (Table 4). The inversely correlations were found between protamine deficiency spermatozoa (CMA3 positive) and concentration (r = -0.33, P = 0.009), motility (r = -0.53, P = 0.00) and normal morphology (r = -0.41, P = 0.002) while the other seminal parameters were less well correlated.

6. Terminal Deoxynucleotidyl Transferase Nick End Labeling (TUNNEL) Assay

In order to determine whether DNA damage is contributed to the protamine deficiency spermatozoa, we performed a TUNNEL assay using flow cytometry. The percentage of DNA damage spermatozoa was significantly higher in Group IV (morphologically normal spermatozoa <4%) compared with Group I (morphologically normal spermatozoa >30%) (33.46±5.46 vs. 17.29±3.79, P<0.05; Table 3). Interestingly, the percentage of DNA damage spermatozoa in Group II (morphologically normal spermatozoa 4-14%) and Group III (morphologically normal spermatozoa 14-30%) were also significantly higher than Group I (morphologically normal spermatozoa >30%) (20.34±2.10, 20.38±1.96 vs. 17.29±3.79, P<0.05). Linear regression analysis revealed that the percentage of DNA damage spermatozoa were negatively correlated with sperm concentration (r = -0.31, P = 0.01; Table 5). In addition, the percentage of DNA damage spermatozoa were also inversely correlated with the percentage of motility (r = -0.46, P = 0.00) and normal morphology (r = -0.29, P= 0.02). There were less correlation between the percentage of TUNNEL positive spermatozoa and volume of ejaculation, age of male and any of the seminal parameters. Of the most important, there was seen to be a high correlation between the percentages of CMA3 positive spermatozoa and TUNNEL positive spermatozoa (r = 0.68, P = 0.00).

Table 3 CMA3 assay and TdT nick end labeling (TUNNEL) assay in the spermatozoa from difference sperm morphological groups, >30%, 14-30%, 4-14% and <4% morphologically normal spermatozoa.

	>30% Normal morphology (N=5)	14-30% Normal morphology (N=14)	4-14% Normal morphology (N=21)	<4% Normal morphology (N=9)
CMA3 positive spermatozoa (%)	16.30 ± 3.21	27.57 ± 2.20	30.79 ± 3.08	42.21 ± 7.30
TUNNEL positive spermatozoa (%)	17.29 ± 3.74	20.34 ± 2.1	20.38 ± 1.96	33.46 ± 5.46

Values represent the mean plus or minus the standard error of mean.

Table 4 Correlation between the percentage of CMA3 positive spermatozoa and sperm concentration, the percentage of motility and the percentage of morphologically normal spermatozoa.

	Concentration	Motility	Normal morphology	TUNNEL positive spermatozoa
No of samples	49	49	49	49
Correlation coefficient	-0.33	-0.53	-0.41	0.68
P-Values	0.01	0.00	0.00	0.00

Table 5 Correlation between the percentage of TUNNEL positive spermatozoa and sperm concentration, the percentages of motility and the percentage of morphologically normal spermatozoa.

	Concentration	Motility	Normal morphology	CMA ₃ positive spermatozoa
No of samples	49	49	49	49
Correlation coefficient	-0.31	-0.46	029	0.68
P-Values	0.01	0.00	0.02	0.00

Discussion

Chromatin has a complex arrangement of DNA and macromolecules with different levels of compaction (24). With progression of spermatogenesis and spermiogenesis, the sperm chromatin begins to lose histones, which are replaced by transition proteins (TP) and then protamines (25-27). At the same time, DNA undergoes the structural changes necessary for the high degree of compaction that effects shrinkage of nuclear volume (9). Hence, damage to DNA itself or aberrations in nuclear proteins can result in abnormal chromatin.

The present study was intended to evaluate chromatin structure, which of the main features of spermatozoa that might profoundly affect fertilization and subsequent development. The results reported in this study indicated that spermatozoa from infertile couples have chromatin anomalies, which could lead to a decrease in fertilization.

In previous studies morphological sperm quality has always been evaluated by light microscopy, sometimes applying Kruger's criteria. However, subcellular sperm anomalies can only be detected by electron microscopy. The ultrastructural examination in spermatozoa from infertile couples showed a higher percentage of immaturity than in controls. Diffuse impairment of spermatogenesis was indicated by incompletely mature

spermatozoa, often in the process of apoptosis. Many binucleate sperm were found in every ejaculate, indicating impairment of germ cell division during spermiogenesis. The percentage of healthy spermatozoa was very low. Interestingly, the higher percentage of spermatozoa with chromatin condensation failures and tail defects was observed in the infertile couples. Numerous principal and end-piece defects and immature forms were also observed. Spermatozoa with incomplete chromatin condensation apparently more often display single-stranded than double stranded DNA (28). Severe chromatin disorders were detected in the majority of infertile couples who had a history of failed IVF. The defects like altered chromatin, signs of decondensation or karyolysis may be due to impaired spermatogenesis (29). Spermatozoa with abnormal tail probably cannot achieve the fertilization area even after acrosome reaction and capacitation (30, 31). Kupker *et al.* suggested that the majority of ultrastructural disturbances of spermatozoa decrease the possibility of successful IVF (29). Intracytoplasmic sperm injection excludes natural selection mechanisms and exposes the risk of transmission of genetic defects (32, 33).

There seems to be a certain association between semen of lower quality, according to conventional measurements (WHO, 1999), and a reduction in a condensation of sperm chromatin. On performing chromatin analysis in the different groups of infertile couples, as describe above, the higher degree of CMA3 positive spermatozoa were found in the infertile couples with morphologically normal spermatozoa 14-30%, 4-14% and <4% with respect to the patients with morphologically normal spermatozoa >30%. Moreover, infertile couples with morphologically normal spermatozoa 4-14% and <4% have CMA3 positive spermatozoa more than a cut-off value (30%) obtained from previous study (20). These anomalies may arise because of fault in mechanism of DNA packaging, including incomplete replacement of histones by protamines, aberration ratios of protamine 1 to protamine 2, high concentrations of non-oxidized SH groups in protamine molecules, or the occurrence of DNA breaks (10, 14, 34-36). Anomalies in DNA packaging, which take place during spermatogenesis, might inevitably affect sperm chromatin decondensation, which is known to be one of the factors related to fertilization failure in ICSI cases (20).

When the different seminal parameters were related, it was found that the best correlations (value of 0.68) corresponded to parameters those are indicative of the state of sperm chromatin, CMA3 positive and TUNNEL positive. This is logical, as these

parameters are completely interrelated, and reflect the evolution of sperm nucleus during spermiogenesis and subsequent maturation. However, when the correlation of sperm chromatin parameters with standard parameters for semen analysis was analyzed, intermediate values (\sim 0.3-0.5) were found, suggesting that these reflect the different physiological processes during spermatogenesis. The standard seminal parameters presented lowest correlation coefficients (\sim 0.2-0.45), which was in agreement with the finding of others (37).

The linear regression analysis performed to determine which seminal variables present the best relationship with the degree of condensation of sperm chromatin, revealed these to be motility, percentage of normal forms in the ejaculate, and the concentration of spermatozoa. Nevertheless, these parameters are only able to predict 50% of the variability observed in the condensation of sperm chromatin, as they reflect biological possesses which differ from those representing nuclear quality (18, 38). The pathological agents such as oxidative stress may affect spermatozoa at different levels at the same time, including mitochondrial function affecting motility, acrosome and membrane functions affecting morphology and vitality (39), and DNA affecting accessibility of PI and, consequently, chromatin related parameters.

Although fertilization is a multifactorial process and many factors might affect fertilization outcome, protamine deficiency has paramount effect on this process. However, once the fertilization barrier is bypassed such as in ICSI cases protamine deficiency has more profound effect on pronucleus formation than sperm morphology (40). In addition, damaged DNA may also contributed failure of sperm decondensation and results in failure of fertilization. Therefore, evaluation of protamine deficiency is essential for prediction of fertilization outcome. In addition, it appears that elimination or reduction of spermatozoa with abnormal chromatin packaging (especially high CMA3 positivity) or abnormal morphology is essential for achieving normal and higher fertilization in IVF and ICSI.

Numerous reports have now established a relationship between abnormal protamine expression and male infertility (10, 34, 41-44). Our data are consistent with these reports and provide convincing evidence for the relationship between protamine deficiency and male infertility. First, the spermatozoa of infertile couples with CMA3 positive have high degree of DNA damaged and reduced motility, sperm concentration,

and normal morphology. Second, we have now shown that protamine deficiency spermatozoa directly correlates with DNA damage and inversely correlates with sperm motility, concentration and normal morphology especially head morphology. Third, most of the infertile couples with CMA3 positive spermatozoa were clinically diagnosed with some form of male subfertility.

There is critical protamine content for proper chromatin packaging and subsequent events in spermiogenesis. The precise nature of this interaction, however, has not yet been elucidated. Recent reports of protamine knock outs indicate that haploinsufficiency of P1 and P2 causes infertility in mice and that mouse P2 deficiency leads to sperm DNA damage and embryo death (45, 46). These data demonstrate that protamines are important components of spermatid differentiation and those aberrations in protamine stoichiometry are related to infertility and may confer defects during spermiogenesis.

Therefore, the evaluation of protamine content may still serve as a valuable clinical diagnostic test for three reasons. First, we have demonstrated that the protamine content highly correlates with concentration, morphology and motility. Second, recent studies have emphasized the importance of sperm DNA damage for proper embryogenesis. Protamine content appears to be critical for proper chromatin integrity evidenced by increased susceptibility of protamine deficient sperm to DNA damage (47, 48). Third, in light of recent concerns about imprinting disease associated with ICSI, human sperm protamines may be of utmost clinical significance even though they do not impair IVF/ICSI pregnancy rates. It is now clear that proper chromatin structure is critical for faithful methylation of imprint genes (49).

Conclusion

In conclusion, we have now shown that infertile couples have a higher load of spermatozoa with protamine deficiency. In addition, protamine deficiency has severely affected DNA integrity and sperm quality. These data highlight the clinical importance of sperm protamines in fertility diagnosis and prognosis. Additionally, identification of the nature of protamine deregulation at the protein expression level serves as a necessary first step to elucidating the underlying causes of abnormal protamine expression in infertile males.

Introduction

Sperm chromatin is a highly compact and complex structure and is capable of decondensation-features that must be present in order for a spermatozoon to be considered fertile. Any form of sperm chromatin abnormalities or DNA damage may result in male infertility. DNA integrity in sperm is also essential for the accurate transmission of genetic information and, in turn, the maintenance of good health in future generations (1).

During spermatogenesis and spermiogenesis of vertebrates, the chromatin undergoes extensive molecular reorganization and condensation that renders it more compact and metabolically inert as all paternal genes are switched off, and the chromatin must be contained within the highly reduced volume of the sperm nucleus (2, 3). Thus, the paternal genome is protected against physical damage and chemical mutagenesis during transport to the site of fertilization (4).

Dramatic biochemical and ultrastructural changes in nuclei occur as mammalian spermatids develop into mature spermatozoa. Histones of spherically shaped nuclei possessing fine granular chromatin are replaced by more basic proteins, the transition proteins, in elongating and condensing nuclei; and these basic nucleoproteins are then replaced by even more basic sperm-specific nucleoproteins, the protamines, in mature spermatids with compact chromatin (5-7).

It has been suggested that the functional status of ejaculated sperm nuclei could result from these complex structural and biochemical alterations. Thus, penetration through the oocyte vestments could be facilitated for elongated spermatozoa with dramatically condensed chromatin (4). Subsequently, the early stages of embryogenesis might depend on nuclear proteins and chromatin organization (8, 9).

This state of chromatin condensation may be altered by various factors, such as a shortage of zinc from the prostate (10), or alterations in protamines (11). Various reports in mammalian species support the hypothesis of a close relationship between nuclear maturity and fertility of ejaculated sperm (12-14).

The assessment of chromatin status is very important when evaluating the ability of spermatozoa to fertilize. Many techniques have been described for the evaluation of

chromatin status, such as optical microscopy (15), electron microscopy (16, 17) and flow cytometry (18). Sperm chromatin defects have been correlated with the reduced ability of spermatozoa to fertilize both in the context of assisted reproduction techniques (19-21) and in the general population (22). Moreover, patients with fertility problems have often been characterized by an increased frequency of spermatozoa with abnormal chromatin (15, 23).

In this study, different groups of patients are examined, both fertile and infertile, in order to analyse the standard parameters of semen analysis and those that depend on the state of sperm chromatin. The ultrastructural charactics, nuclear shape and chromatin texture of human spermatozoa are analyzed through the use of transmission electron microscopy (TEM). Size, shape, and chromatin texture parameters were found to be salient indicators of stage-related nuclear transformations from early spermiogenesis to the end of epididymal transit. Thus, it is possible to observe differences between patient groups. The protamines in the nucleus of both fertile and infertile spermatozoa were analyzed by using CMA3 assay. Furthermore, the distribution of transition protein and protamines in spermatozoa from fertile in infertile were observed to clarify whether it is related to reproductive capacity or not. The data obtain from this study might be serve as a diagnostic tool in clinical practice for IUI, IVF and ICSI treatments

Literature Review

The male reproductive system encompasses the anatomical structures and physiological functions that produce mature spermatozoa. This system has two theoretically distinct, but interrelated, aspects: fertility and virilization ("maleness"). To briefly summarize, the processes of sex determination and embryonic development produce a male child, setting the stage for the virilization and onset of fertility that begin with puberty. As with female reproduction, the brain, specifically the hypothalamus, signals the pituitary gland to secrete LH and FSH in a pulsatile pattern characteristic of adulthood. LH and FSH have specific functions in the testis. FSH stimulates male germ cells to develop into mature sperm, a process called spermatogenesis. LH stimulates testis accessory cells, called Leydig cells, to produce sex steroids, especially testosterone, through the process of steroidogenesis. Male hormones are needed for optimal sperm production, as well as for sexual function, healthy blood and bones, and general well being.

Sperm Production: Spermatogenesis

Spermatogenesis is a complex cellular process responsible for the production of a large numbers of spermatozoa. In most vertebrates this process takes place within the narrow and highly coiled seminiferous tubules, each having a central fluid-filled lumen lined by the epithelium composed of germinal cells and somatic cells, the Sertoli cells, which support and nourish the germ cells (24).

Generally, spermatogenesis in animals can be subdivided into three main phases, each involving classes of differentiating germinal cells (24, 25).

First phase: The proliferation and renewal of spermatogonia. The spermatogonia are stem cells located at the base of the seminiferous epithelium. They divide by mitosis to yield a pool of renewing spermatogonia and differentiated spermatocytes, which gradually move away from the basement membrane of the epithelium (26).

Second phase: Meiosis. Spermatocytes are unique in their ability to undergo two successive reductions or meiotic divisions that produce the spermatids, which have exactly half the number of chromosomes (27). Spermatids are said to be haploid while spermatogonia and somatic cells are diploid. In males, the first meiotic division, or

meiosis I, begins during the G_2 phase of the cell cycle prior to the onset of the leptotene of prophase I in primary spermatocytes. During this period known as the pre-leptotene phase of meiosis I, chromosomes of the primary spermatocyte are replicated. Thus, the diploid genome of the primary spermatocyte has already been doubled during the G_2 phase of the preceding cell cycle. All primary spermatocytes entering meiosis I as tetraploid and posses two sets of chromosomes, or dyads, each of which comprise of two sister chromatids joined at the centromere (28).

Throughout the remaining period of meiosis, there is no further synthesis of DNA (29). During the pachytene stage of prophase I, segments of genetic information are exchanged between homologous chromatids through the process of crossing-over. When telophase I is completed, each primary spermatocyte yield two diploid secondary spermatocytes containing recombined dyadic chromosomes (27).

Prior to the onset of meiosis II there is no replication of DNA or cellular growth, and the secondary spermatocytes begin to divide almost immediately. The dyadic chromosomes, which have been segregated into secondary spermatocytes during meiosis I, are separated into sister chromatids during meiosis II (27). With the completion of telophase II, each sister chromatid, along with its own centomere, is segregated into a different spermatid. When meiosis is completed, each of these sister chromatid becomes a chromosome, all spermatids remain connected by cytoplasmic bridges and are partially embedded in the cytoplasm of Sertoli cells (28).

Third phase: Spermiogenesis. Spermiogenesis is the process through which round spermatids mature into spermatozoa, fully mature sperm capable of swimming. The nucleus progressively elongates as its chromatin condenses and gradually takes on a variety of shapes that characterize the heads of spermatozoa of various species (30). The Golgi apparatus of a developing spermatid elaborates numerous carbohydrate-rich membrane bound vesicles known as proacrosomal granules (31). These granules fuse to form a single large acrosomal vesicle that contains a dark-stained acrosomal granule. As the spermatid continues its differentiation, the acrosomal vesicle migrates to the vicinity of the nucleus where it transforms into the anterior end of the spermatid. Once locating near the nucleus, the membrane of the acrosomal vesicle grows over the anterior end of the nucleus and produces a cap-like structure known as the acrosome (32). The mature acrosome is a specialized lysosome-containing carbohydrates and

hydrolytic enzymes: especially hyaluronidase and proteases, which are necessary for the sperm to undergo the fertilization process with the ovum (33). Following the completion of the last meiotic division in early spermatids, the centrioles begin to migrate to the posterior pole opposite to that occupied by the acrosome. The distal centriole act as a basal body and establishes the microtubule organizing center (MTOC) necessary for the growth of the flagellar axoneme. In most vertebrates, one or both of the centrioles degenerate during development of axoneme. However, in mammals, they may persist as the neck region of the mature spermatozoa (34). As the nucleus elongates, the main bulk of the cytoplasm with the mitochondria migrates toward the base of the flagellar axoneme, and the latter form the mitochondrial sheath within the newly formed midpiece, which constitute the energy yielding organelle for the spermatozoon (30). The bulk of cytoplasm of a spermatid is eventually discarded as the residual body, which is phagocytosed and eliminated from the seminiferous epithelium by Sertoli cell (35). Once cytological transformation is complete, spermiation begins (36). This is the process by which immature spermatozoa in the last step of spermiogenesis are detached from their syncytium and released from Sertoli cells cytoplasm into the lumen of the seminiferous tubule. Once free within the lumen of seminiferous epithelium, immature spermatozoa will continue to develop and mature during its transit through the epididymis (28).

Chromatin Organization during Spermatogenesis in Mammalian Male Germ Cells

Spermatogonia divide by mitosis and differentiate until they become primary spermatocytes, which will be arrested at leptotene stage until puberty. At puberty, primary spermatocytes begin to divide by meiosis and go into prophase stage which is subdivided into six phases, i.e., leptotene, zygotene, pachytene, diplotene, diakinesis and metaphase.

In the leptotene stage, the chromosomes appear as thin, delicate filaments, which are attached to the nuclear envelope at the periphery and intertwined together in the center. Each chromosome is composed of two sister chromatids. In the subsequent zygotene stage, there is intimate pairing of homologous chromosomes; in human each of 23 homologous chromosomes are paired by trilaminar structures called the synaptonemal complexes (37). In the pachytene stage, there are exchanges of genetic material between homologous chromosomes mediated by the synaptonemal complex. In the

diplotene stage, desynapsis occurs and the areas where there have been exchanges of genetic material are clearly seen at the connecting sites called chiasmata (37, 38). In the final stage, diakinesis, the separated chromosomes become condensed into large blocks. The cells then proceed into metaphase where the paired chromatids are aligned at the equatorial plate. Chiasmata separate and the homologous chromosomes move to opposite poles of the cell during anaphase. In telophase, cytokinesis occurs and two separate daughter cells are derived. At the end of this first meiotic division, the cells have differentiated into secondary spermatocytes (27).

There is a very short interphase between the first and second meiotic divisions, and no DNA synthesis occurs during this period. Almost immediately, the second division begins with the secondary spermatocyte progressing from prophase through metaphase, anaphase and telophase. The second division closely resembles mitosis metaphase where there is a separation of sister chromatids along the centromere. At the end of the second division, a secondary spermatocyte gives rise to two spermatids. The spermatid undergoes a dramatic metamorphosis, a process called spermiogenesis, during which its chromatin becomes increasingly condensed until the highly packed chromatin in the spermatozoon appears.

One of the last structural changes to occur during spermiogenesis in mammals is the repackaging of the spermatid genome. This process is initiated by the synthesis and deposition of a highly basic nuclear proteins called protamines in late step spermatids (1, 39, 40); and this is accompanied by a dramatic change in the chromatin condensation (41, 42). Subtle changes in the structure and semicondensed state of chromatin could be observed prior to this time, but the final and most dramatic event in DNA compaction is induced when protamines bind to DNA and displaces all other basic nuclear chromatin proteins. It has been assumed that this process of DNA condensation must play a critical role in reprogramming the sperm genome, since changes in the proportion of particular protamines, and the alterations that disrupt histones removal appear to lead to male infertility (10).

Chromatin Organization in Somatic Cells

Nuclear DNA in somatic cells of vertebrates is organized in a hierarchy of structures, leading to the packaging of 2 meter long DNA into a nucleus with a diameter as small as of 5-10 µm (43). The first order structure of DNA is the 2 nm right-handed double helix. The second level of DNA organization is the nucleosomes, each of which is composed of core dimeric histones, H2A, H2B, H3, and H4, forming the protein center of the repeating structural unit of the chromatin (44). The nucleosome consists of 146 base pairs of DNA wrapping 1.65 turns around the histone octamer core arranged as an H3-H4 tetramer complex and two H2A-H2B dimers positioned on each face of the tetramer (43). Histone H1 binds to linker DNA that joins the nucleosomes together (45). It was previously demonstrated that chromatin in low ionic strength solutions had an extended "beads-on-a-string" conformation (the beads being the nucleosome) (46). The third level of chromatin structure is that of the 30 nm filament, which is formed by the coiling up in solenoid pattern of the 10 nm histone-DNA fibers, with at least six nucleosomes per turn (47). This folding is dependent upon the interaction of histone H1 with the N-terminal tails of the core histones, which stabilizes the 30 nm fiber (48, 49). In chromosomes, the 30 nm fibers form loop domains which are threaded at their bases to the non histone proteins called scaffold proteins, which are essentially serving as the core structure of each chromosome (50).

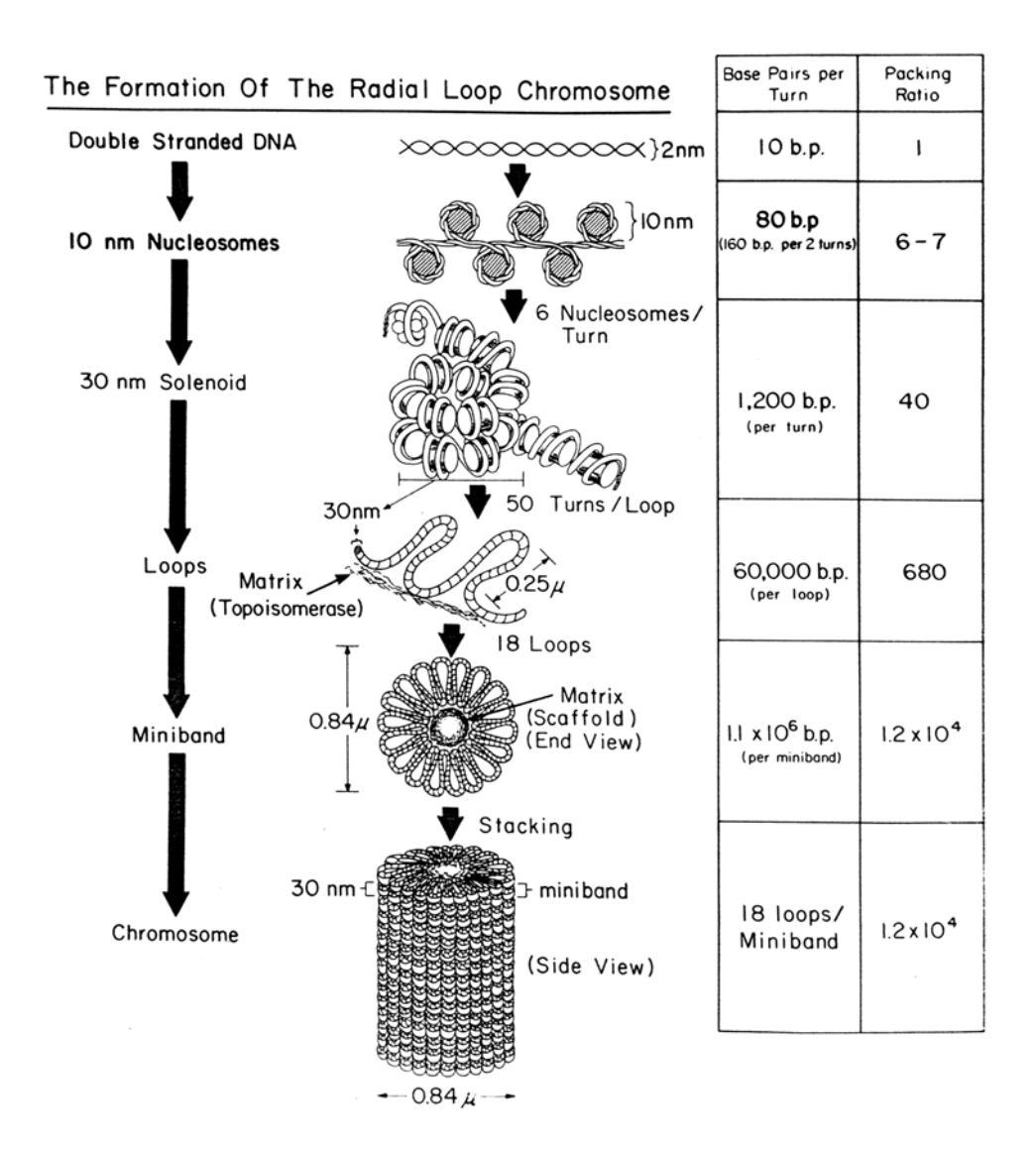


Figure 1 Schematic of the levels of organization of chromatin and their folding into a chromosome. Approximately 160 bp of 2 nm DNA helix is wound twice around the histone octamers to form the 10 nm nucleosomes. These nucleosomes form a "beadson-a string" fiber, which winds in a solenoid fashion with 6 nucleosomes per turn to form the 30 nm chromatin filament. The 30 nm filament forms the 60 kbp DNA loops that are attached at their bases to the nuclear matrix structure. The loops are then wound into the 18 radial loops that form a miniband unit or 1 turn on the chromatid. The minibands are continuously wound and stacked along a central axis to form each chromatid. (A courtesy of Getzenberg *et al.*, 1991)

DNA Packaging in Mammalian Male Germ Cells

Unlike the somatic cells, the sperm nucleus is too small to have sufficient volume to contain DNA in the nucleosomal organization. Therefore, the sperm of most vertebrates, especially mammals, are known to posses a unique type of DNA packaging by virtue of the unique associations among the DNA, nuclear matrix, and sperm nuclear proteins (protamines) (51). The DNA of spermatozoa is extremely compact, being about six folds more than mitotic chromosomal DNA (52, 53). Accompanying this compaction is the extensive structural reorganization of DNA, accomplished by the sequential replacement of somatic histones by nuclear packaging proteins, the transition proteins, and the protamines (2, 40). In addition to the normal complements of histones present in somatic cells and in premeiotic male germ cells, the nuclei of primary spermatocytes also contains a vast array of testis-specific histones, including variants of histone H2A, H2B, and H1 invariably named TH2A, TH2B and TH1 (54). In mammals during spermiogenesis, somatic and testis specific histones are replaced by several transitional proteins (TP), small lysine- and arginine-rich proteins that help transform the nucleosomal chromatin into smooth condensed chromatin fibers (3, 55, 56). As the nucleosomal organization disappears in the middle stages spermatids, transcription terminates, despite the finding that late-stage male germ cells contain 1000 folds more TATA-binding protein than somatic cells (57). During the last stages of spermatids, the protamines, small basic nuclear proteins containing over 60% arginines, replace the transition proteins and facilitate the molecular remodeling and species-specific compaction of the male genome within the differentiating spermatid nucleus (2).

Protamines are relatively small, highly basic proteins found in spermatozoa of most vertebrates. There are two types of protamines, i.e. protamine-1, which is found in nearly all mammals (58), and protamine-2, which is confined to relatively few species that include human (59), mouse (60), and stallion (61). The protamines can bind to the minor groove of DNA. Their positive charges are believed to neutralize the negatively charged phosphate groups in the DNA backbone (51). This permit one strand of DNA-protamine to fit into the major groove of another DNA-protamine strand, so that the DNA-protamine strands would be packaged side-by-side resulting in a stacked linear array of DNA (4, 9, 51) (Fig. 2). Such lateral growth of each DNA protein fibers could explain the pattern of chromatin condensation in rodent (rat, mouse, hamsters) spermatozoa, where the nucleosomal type chromatin fibers are straightened up to form

40-50 nm fibers in middle stage spermatids (step 10-11 in rat). These fibers then grow larger up to 100 nm, and finally are fused to form highly compact and electron opaque chromatin mass. The protamine-associated male haploid genome has been estimated to be approximately six folds more highly condensed than that of somatic cells (52). Furthermore, protamines also contain numerous cysteine residues which are used to generate strong disulfide (-S-S-) cross links between adjacent protamine molecules and further stabilizing a highly compact structure of chromatin by intermolecular and intramolecular covalent disulfide bonds between protamines (4). Thus, the DNA in sperm nucleus can be tightly packaged in a very small volume.

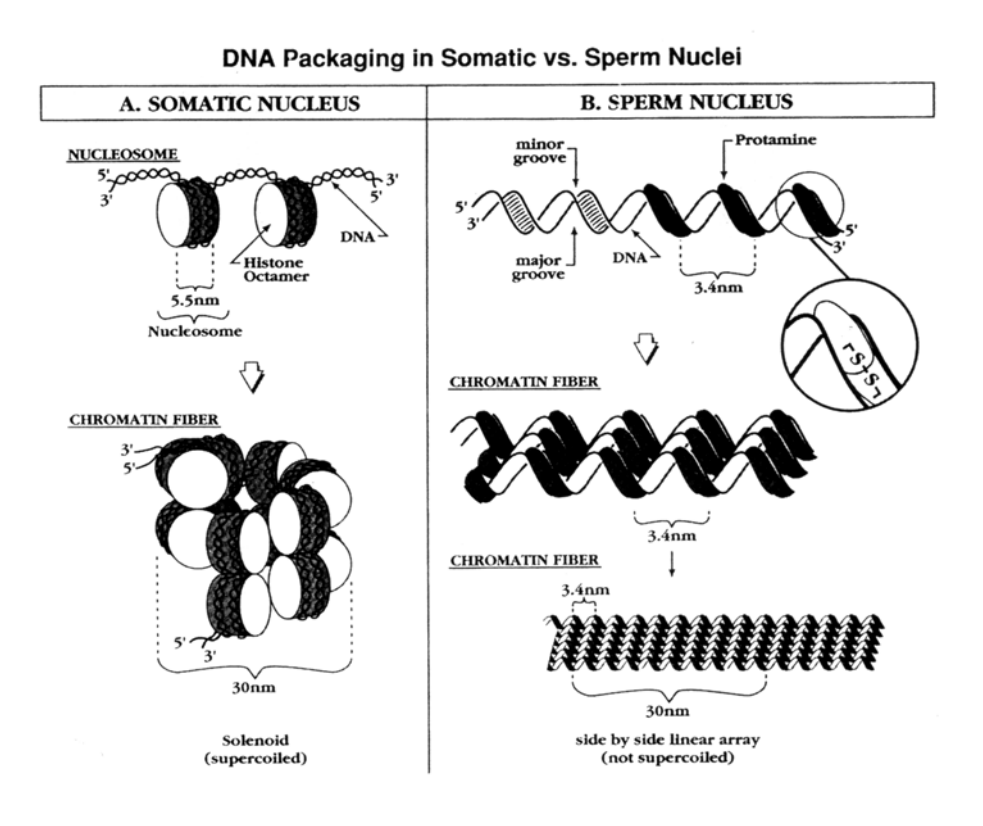


Figure 2 DNA packing structures in somatic vs. sperm nuclei. (A) Diagram illustrating how histones bind DNA by coiling it into solenoids. The coiling of DNA around histone octamers cause eukaryotic DNA to be negatively supercoiled, in vivo. (B) Diagram illustrating protamines bind to minor grove of DNA and permit one strand of DNA-protamine to fit into the major groove of another DNA-protamine strand and then package the DNA into linear, side-by-side arrays. (A courtesy of Ward and Coffey, 1991)

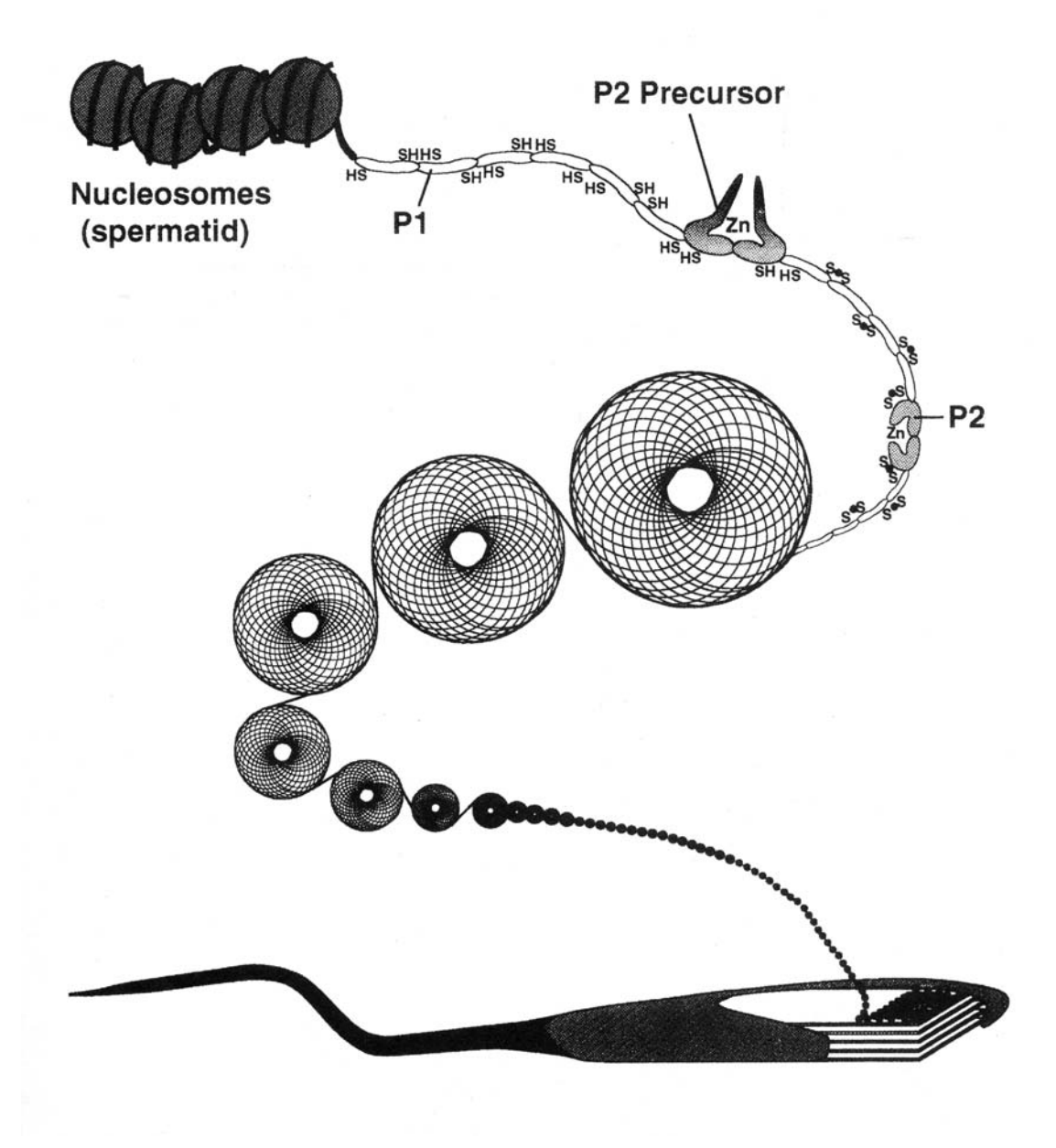


Figure 3 The process of chromatin reorganization in the spermatid is initiated by the synthesis and binding of P1 and P2 to DNA. This displaces all the existing chromatin proteins and coils the DNA into toroidal structures containing about 50 kbp of DNA. Each sperm nucleus may contain approximately 50,000 toroids. (A courtesy of Balhorn *et al.*, 1999)

Alternatively, recent studies of the binding of protamines to DNA illustrated that the charge-neutralized sperm DNA could be coiled up by individual nucleoprotamine fiber to form toroidal structure (~ 50-kb DNA per toroidal unit) with diameter 60-100 nm and thickness about 20 nm (62, 63). These tori are believed to form the fundamental packaging units of chromatin in bull (64), human (62), and primate (61) spermatozoa. Then, the coiled DNA continues to form a toroidal loop defined by the persistence of about 500 base pairs along the length of DNA (65), and the torus grows in size as subsequent loops bind adjacent to the previous ones. Eventually, each toroid may contain up to 60 kilobase of DNA. The final result is that a very compact nucleoprotamine complex could be tightly packed inside a very small volume of sperm nucleus (Fig. 3). The intermolecular and intramolecular disulfide cross-links between the cysteine-rich protamines are responsible for the compaction and stabilization of the sperm nucleus, and it is thought that this nuclear compaction is important to protect the sperm genome from external stresses such as oxidation or temperature elevation in the female reproductive tract (66). Paradoxically, the protamines and associated sulfhydryl groups may have an important role in the process of decondensation during fertilization (66).

Interestingly, the DNA in human sperm chromatin is partitioned into both a nucleohistone and a nucleoprotamine fraction with 15% of the DNA is packaged by histones in sequence-specific areas (67). The histone-bound DNA sequences are less tightly compacted (and hence, more likely to be readily decondensed early in fertilization). Presumably these DNA sequences and/or genes may be involved in fertilization and early embryo development (51, 67). The retained histones are associated with telomeric sequences that may be among the first structures in the sperm nucleus to respond to oocyte signals for pronucleus formation (68) .Telomere-microtubule complexes are formed in cells and may be involved in the movement of the male pronucleus (69). It is unknown whether the sequence-specific chromatin packaging is preserved in spermatozoa of infertile men, but a significant percentage of spermatozoa in these men possess a greater proportion of retained histones (70).

Human Male Infertility

Approximately 15% of couples attempting their first pregnancy meet with failure. Most authorities define these patients as primarily infertile if they have been unable to achieve a pregnancy after one year of unprotected intercourse. Conception normally is achieved within twelve months in 80-85% of couples who use no contraceptive measures, and persons presenting after this time should therefore be regarded as possibly infertile and should be evaluated. Data available over the past twenty years reveal that in approximately 30% of cases pathology is found in the man alone, and in another 20% both the man and woman are abnormal. Therefore, the male factor is at least partly responsible in about 50% of infertile couples.

Etiology of sperm DNA damage

The etiology of sperm DNA damage, much like male infertility, is multifactorial and may be due to intratesticular, post-testicular, or external factors. Sperm DNA damage is clearly associated with male infertility (and abnormal spermatogenesis), but a small percentage of spermatozoa from fertile men also possess detectable levels of DNA damage (71, 72). It is unknown whether a single factor or multiple factors (possibly acting in a cascade) are responsible for sperm DNA damage. The following is a list of potential etiologic factors: protamine deficiency; apoptosis; drugs, chemotherapy, and radiotherapy; ROS; cigarette smoking; post-testicular factors; and varicoceles.

Protamine deficiency

A frequent abnormality of sperm chromatin is a relative or complete deficiency of sperm protamines (the principal sperm nuclear proteins) (70). An important subset of infertile men (~5% to 15%), but not of fertile men, possesses a complete protamine deficiency, and some of the affected individuals have a genetic mutation in the protamine gene cluster (70). Although studies on transgenic animal models with targeted protamine deficiency suggest a link among protamine deficiency, sperm DNA damage, and poor fertilizing capacity at in vitro fertilization (IVF), no such associations have been studied in humans (73). A single case report indicated that a febrile illness can cause a transient increase in the nuclear histone/protamine ratio and associated abnormalities of sperm chromatin structure (74).

Apoptosis

Apoptosis or programmed cell death during normal mammalian spermatogenesis results in the destruction of up to 75% of potential spermatozoa (75). It is the selective apoptosis of these early germ cells that prevents overproliferation of germ cells and selectively aborts abnormal spermatozoal forms (75). This allows the fixed Sertoli cell population to support adequately a specified number of germ cells that are undergoing clonal expansion through several rounds of mitosis. It has been postulated that this clonal expansion is specifically controlled by the production of the cell surface protein Fas (76). This mediator of sperm cell apoptosis allows the Fas ligand to bind to Fas and induce cell death.

It has been proposed that some of the spermatozoa with DNA damage have initiated and then subsequently escaped apoptosis (abortive apoptosis) (77). This theory has been challenged by other investigators (78). Some controversy exists as to whether spermatozoa have the capacity to undergo apoptosis, because these specialized cells have no real capacity for the controlled production of new proteins (through transcription and/or translation).

Drugs, chemotherapy, and radiotherapy

Young men with cancer (e.g. Hodgkin's lymphoma and testicular cancer) typically have poor semen parameters before cancer-specific therapy, experience cumulative dose damage, and are often rendered sterile after therapy. Before therapy, these men may already have high levels of sperm DNA damage (significantly greater than that seen in fertile men) (79).

It has been shown that systemic chemotherapy is associated with sperm DNA damage (79, 80). The rapidly dividing germinal epithelium of the testis is a natural target for cytotoxic medications. Both radiotherapy and chemotherapy inflict similar damage and both are dependent on the duration of exposure and the dose of the exposure (79-81). The recovery of spermatogenesis may occur months to years after therapy, but evidence of sperm DNA damage will often persist even longer (81).

Reactive oxygen species

Although low levels of ROS in semen may be important for normal sperm maturation, studies have shown that high levels of ROS can adversely affect multiple sperm functions and sperm DNA integrity (82, 83). High levels of ROS are detected in the semen of ~25% of infertile men but not in the semen of fertile men (84). We have found that the retention of cytoplasmic droplets (a morphologic feature associated with ROS production and a sign of sperm immaturity) is positively correlated with sperm DNA damage (85). Leukocytospermia is also associated with high levels of sperm DNA damage, likely secondary to elaboration of ROS by these cells. ROS may also cause hypercondensation of the sperm nucleus as a result of excessive oxidation of protein sulfhydryl groups.

Cigarette smoking

Studies have shown that cigarette smoking is associated with lower sperm counts and motility and an increase in abnormal forms (86). It has been postulated that smoking causes increased leukocyte-derived ROS production, with adverse effects on developing and mature sperm (87). It has been shown that the level of sperm DNA damage is greater in smokers than in nonsmokers (87).

Post-testicular factors

Sperm DNA damage may also be caused by post-testicular and systemic factors. Post-testicular, genital tract infection and idiopathic genital tract inflammation, both resulting in leukocytospermia, have been associated with increased numbers of immature germ cells in semen. The immature sperm cells of these men have been examined and found to have increased levels of DNA damage compared with the sperm of normal male donors. A febrile illness has been shown to cause an increase in DNA damage and the histone/protamine ratio in these immature spermatozoa (74).

Varicoceles

Varicoceles have recently been associated with sperm DNA damage (88). The level of sperm DNA damage is related to the high levels of oxidative stress found in the semen of these infertile men (89). We have shown that varicoceles are associated with the

abnormal retention of sperm cytoplasmic droplets (a morphologic feature associated with high levels of semen ROS) and that these retained droplets are correlated with sperm DNA damage in these infertile men (85, 89).

In conclusion, mammalian fertilization involves the direct interaction of the sperm and oocyte, fusion of the cell membranes, and union of male and female gamete genomes. The completion of this process and subsequent embryo development depend in part on the inherent integrity of the sperm DNA. A threshold of sperm DNA damage (i.e., DNA fragmentation, abnormal chromatin packaging, protamine deficiency) appears to exist beyond which fertilization and embryo development are impaired. Clinical evidence has now shown that human sperm DNA damage may adversely affect reproductive outcomes and that the spermatozoa of infertile men possess substantially more DNA damage than the spermatozoa of fertile men. However, our understanding of the etiologies of sperm DNA damage and the full impact of this sperm defect on reproductive outcomes in humans remains rudimentary.

One of the most interesting research areas for understanding the DNA damage that affect the fertilizing capability is the packaging of DNA, DNA - protein complexes, in the nucleus of human spermatozoa. Only limited amount of information is available on the packaging of DNA in spermatozoa of infertile men. Thus, one of the purposes of this project is to study the ultrastructural characteristics of chromatin packaging in infertile spermatozoa, as well as to investigate the composition and distribution of basic nuclear proteins in the nucleus of infertile spermatozoa, especially with regards to protamines. The results obtains from this study will provide the basic knowledge on abnormal DNA packaging in the infertile spermatozoa that might be affect the fertilizing capability of spermatozoa. At molecular level, it will provide the understanding of how paternal genome is abnormally packaged in an infertile person and the pattern could be used as one criterion in diagnosis of human infertility.

Objectives

1. Overall objective

The overall objective of this research is to investigate the relationship between chromatin packaging, sperm quality and DNA integrity in spermatozoa from infertile couples.

2. Specific objectives

- 2.1 To study the ultrastructure of spermatozoa from infertile couples by transmission electron microscopy.
- 2.2 To study the chromatin packaging in the nucleus of spermatozoa from infertile couples by transmission electron microscopy.
- 2.3 To study the distribution of transition protein and protamines in the nucleus of spermatozoa from infertile couples.
- 2.4 To evaluate the protamine content in nucleus of spermatozoa from infertile couples.
- 2.5 To study the DNA integrity in the nucleus of spermatozoa from infertile couples.
- 2.6 To deduce the relationship between the pattern of chromatin organization, the basic nuclear protein profiles and the reproductive capacity.

Materials and Methods

1. Preparation of Semen Samples

The study was approved by the Ethical Committee of Faculty of Medicine, Thammasat University. All subjects participated in the study after giving written informed consent. Semen samples were obtained from a total of 49 patients attending the Center for Assisted Reproduction and Embryology, Thammasat University Hospital, Thailand for diagnostic semen analysis. Semen samples were obtained by masturbation after at least 3 days of sexual abstinence, and collected in sterile plastic containers. Semen samples were allowed to liquefy for 30 min at 37°C for further studies.

2. Preparation of Human Spermatozoa for Transmission Electron Microscopy (TEM)

The spermatozoa were fixed in the solution of 4% glutaraldehyde plus 2% paraformaldehyde in PBS, pH 7.4, at 4°C for 1 hour, and then the specimens were washed in three changes of the same buffer in order to remove the fixatives, followed by post fixation in 1% osmium tetroxide in the same buffer for 30 minutes. Then the specimens were washed again in three changes of the same buffer. After fixation, specimens were dehydrated through an increasing concentrations of ethyl alcohol at 50%, 70%, 90%, consecutively for twice, 5 minutes at each concentration, at 95%, for twice, 10 minutes each, and at 100%, for 3 times, 15 minutes each, at 4°C, and for 3 times, 20 minutes each, at room temperature, cleared in two changes of propylene oxide, for 15 minutes each, infiltrated in the mixtures of propylene oxide and Araldite 502 resin at the ratios of 2:1 for 1 hour, and 1:2 overnight; then in pure Araldite 502 resin for at least 6 hours, and finally polymerized at 30°C, 45°C and 60°C for 24, 48 and 48 hours, respectively.

3. Electron Microscopy Study

Thin sections with an interference color of silver to silver-gold (about 60-90 nm thick) were cut with diamond knife on a Porter-Blum MT-2 ultramicrotome. The sections were picked up on uncoated 300-mesh copper grids, air dried and stained by floatation on saturated aqueous uranyl acetate in the dark for 30 minutes, then rinsed with several changes of distilled water, and the excess water blotted off with Whatmann filter paper.

The sections were further stained by floatation on saturated aqueous lead citrated for 30 minutes, rinsed with several changes of CO_2 -free distilled water, and the excess water blotted off with Whatmann filter paper and air dried. The sections were then observed with a Philips CM 100 TEM at 80 kV.

4. Preparation of the Spermatozoa for Immunoelectron Microscopic Study

For immunoelectron microscopy, human ejaculated spermatozoa were fixed with 4% paraformaldehyde plus 0.2% glutaraldehyde in PBS pH 7.4 for 1 hour at 4°C. The fixatives were removed by washing three times in the same buffer, for 15 minutes each. Subsequently, the spermatozoa were dehydrated by passage through increasing concentrations of ethanol at 70%, 80%, 90%, twice for each concentration, for 30 minutes each. Then infiltrated in the mixture of LR White resin (London Resin, Berkshire, UK.) and 90% alcohol at the ratio of 1:1 for 2 hours, and then in pure LR White resin for overnight before being embedded in the fresh batch of LR White resin. Anaerobic polymerization was performed at the temperature lower than 50°C for 24 hours.

5. Immunogold Electron Microscopic Analysis

LR White-embedded ultrathin sections (about 60-90 nm thick) of human spermatozoa were cut with diamond knive on a Porter-Blum MT-2 ultramicrotome and mounted on 300-mesh nickel grids. The applications of various solutions to the tissues sections were done by floating the grids, tissue-side down, on drops of the relevant solutions. The sections were first blocked for 15 minutes in 0.15 M glycine in 0.05 M PBS, pH 7.4, at room temperature, followed by 4% BSA in 0.05 M PBS, pH 7.4, for 2 hours at 4°C. The sections were then incubated for 2 hours at 4°C with one of the primary antibodies (mouse anti-human protamine 1 antibody, mouse anti-human protamine 2 antibody, and rabbit anti-human TP) at dilution of 1:100 in 0.05 M PBS, pH 7.4, plus 1% BSA (w/v). After extensive washing with 0.05 M PBS, pH 7.4, plus 0.05 % Tween 20 (v/v), the sections were incubated for 30 minutes with corresponding secondary antibodies coupled with 10 nm colloidal gold particles at dilution of 1:200 in 0.05 M PBS, pH 7.4, plus 1 % BSA (w/v). The sections were then extensively washed in 0.05 M PBS, pH 7.4, plus 0.05 % Tween 20 (v/v), followed by distilled water before being dried. The sections were then counterstained with uranyl acetate and observed under a Philips CM

100 TEM at 80 kV. For negative controls, the sections were treated as above with the omission of the primary antibodies to assess the specificities of the immuno-stainings.

6. Semen Analysis

After liquefaction of the semen, sperm parameters (volume of ejaculation, pH, sperm concentration, percentage of motility, and motion characteristics) were evaluated according to World Health Organization (WHO, 1999) guidelines using a computer-assisted semen analyzer (CASA) and Makler counting chamber.

7. Evaluation of Sperm Morphology

Following preparation of smears, slides were allowed to air dry at room temperature for 20 min and fixed in equal part of 95% ethanol and ether for 15 minutes. Fixed smears were stained with the Harris' hematoxylin for 2 minutes, and then the slides were washed with running tap water for 5 minutes. Then the slides were further stained with orange G6 for 2 minutes. After staining, the slides were washed with two changes of 95% ethanol for 15 seconds. The slides were allowed to dry overnight, mounted and kept in a dark and cool place until analysis. Bright field illumination and a magnification of 100X under an oil immersion objective were used for evaluation. A total of 200 spermatozoa were scored per slide for normality according to the Kruger Strict criteria (90, 91).

8. Chromomycin A3 (CMA3) Assay

Semen samples were washed in Ca²⁺ and Mg²⁺ -free phosphate-buffered saline and were fixed in methanol/glacial acetic acid 3:1 at 4 °C, for 5 min. Following preparation of smears, slides were allowed to air dry at room temperature for 20 min. For CMA3 staining, each slide was treated with 100 µl CMA3 solution for 20 min. The CMA3 solution contained of 0.25 mg/ml CMA3 (Sigma Chemicals, St Louis, MO, USA) in McIlvane's buffer (7 ml citric acid 0.1M + 32.9 ml Na₂HPO₄7H₂O 0.2M), pH7.0, supplemented with 10 mmol/l MgCl₂. Slides were rinsed in buffer and mounted with Antifaded (Vectra Shield). Microscopic analyses of the slides were performed on a fluorescent Nikon Eclipse 600 microscope (Tokyo, Japan), with appropriate filters (460-470 nm). A total of 200 spermatozoa were randomly evaluated on each slide. Evaluation of CMA3 staining was carried out by distinguishing between bright yellow stained spermatozoa (CMA3 positive) and dull yellow stained spermatozoa (CMA3 negative). A

clear distinction existed between CMA3 positive and negative spermatozoa, since CMA3 positive spermatozoa revealed an intensive bright fluorescent yellow appearance.

9. Terminal Deoxynucleotidyl Transferase Nick End Labeling (TUNNEL) Assay

Terminal deoxynucleotidyl transferase (TdT) nick end labeling (TUNNEL) assay provides a direct measure of DNA breaks. TUNNEL assay (APO-DIRECT Kit, BD Biosciences) was executed following the manufacturer's specification. Briefly, spermatozoa were fixed in 1% (w/v) paraformaldehyde in PBS (at a concentration of 1-2x10⁶ cells/ml) for 30 min at 4 °C. After centrifuge at 300g for 5 min, the spermatozoa were washed with PBS 3 times, 5 min each. Subsequently, the spermatozoa were resuspended in 70% (v/v) ice cold ethanol at concentration to 1-2x10⁶ cells/ml and stored at -20 °C until use. For detection, the spermatozoa were washed in 1 ml of Wash buffer 2 times and incubated in Staining solution (10 μ l reaction buffer, 0.75 μ l TdT enzyme, 8 μ l FITC-dUTP, 32.25 μl distilled water) for 60 min at 37 °C. At the end of incubation time, the spermatozoa were washed with Rinse buffer 2 times, 5 min each. Thereafter, the pellet of spermatozoa was resuspended in 0.5 ml of PI/RNase staining buffer and incubated in the dark for 30 min at room temperature. Spermatozoa were analyzed within 3 hours using FACSCalibur[™] flow cytometer. (Becton Dickinson) equipped with a 488 argon laser as the light source. The resulting fluorescence was detected with a 580/30 bandpass filter and quantified using Cell Quest software (Becton Dickinson). A minimum of 5,000 spermatozoa per sample were analyzed.

10. Statistical Analysis

Data were presented as mean ± standard error of the mean (SEM) for the number of individual seminal parameters identified. The ANOVA test was used to assess the significance of differences between observed data. *P*-value of < 0.05 was considered to be statistically significant. Seminal parameters were correlated to CMA3 and TUNNEL assay using Spearman's ranked correlation

Results

1. Ultrastructure of Spermatozoa from Infertile Couples

The ultrastructural analysis showed heterogeneity in sperm nuclear morphology with some spermatozoa showing the round nucleus and other sperm showing a more elongated nucleus (Fig. 4-6). The disruption in chromatin condensation, identified by a coarse granular pattern and contains numerous vacuoles, in the spermatozoa from infertile couples is observed (Fig. 6). In addition, spermatozoa from infertile couples tend to have multiple defects involving: acrosomal disorders, cytoplasmic residues, lack of peripheral microtubules, additional axoneme and midpiece abnormalities (Fig. 6). As far as immaturity is concerned, the nuclei were irregularly shaped, generally elliptical or spherical, with uncondensed chromatin (Fig. 5) and residual cytoplasmic droplets surrounding the nucleus or midpiece regions (Fig. 6). Binucleated spermatozoa are generally observed. Axonemal structure is often altered, lacking central microtubule, and some doublets has incomplete or absent dynein arms (Fig. 6). The tail is often rolled up into cytoplasmic droplets with a disorganized fibrous sheath and accessory fibers, mitochondrial helix is badly assembled.

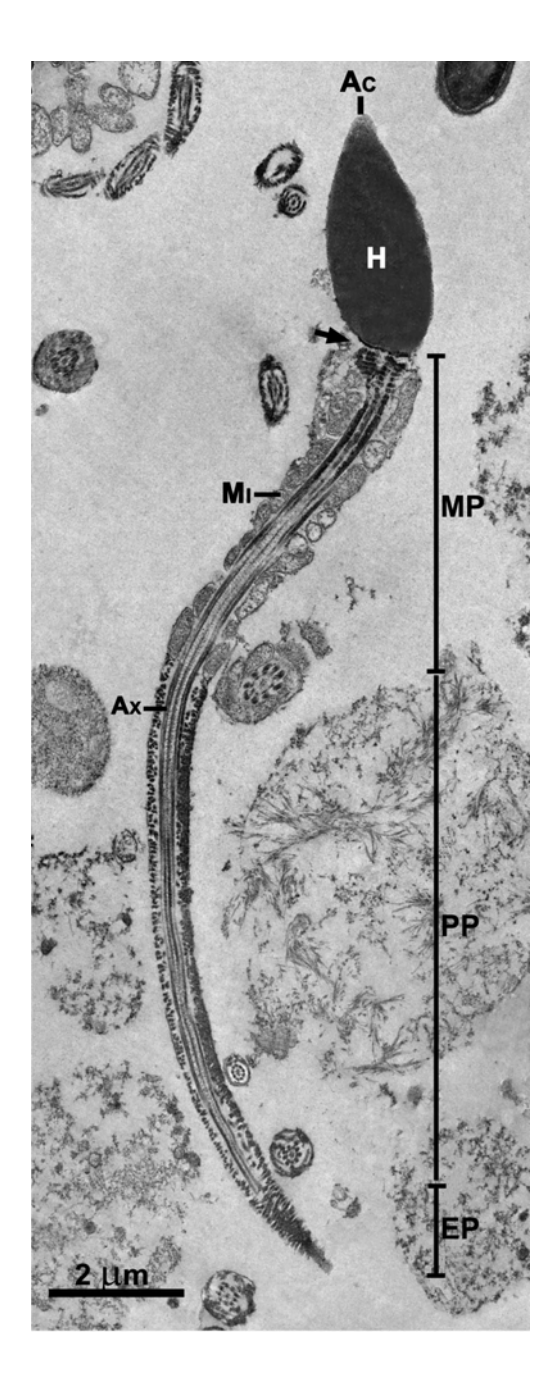


Figure 4 TEM micrograph of longitudinal section of human spermatozoa demonstrating the sperm head (H) with very long tail about 5-6 times the length of the head. The lotus shaped nucleus contains the completely condensed chromatin. The acrosome (Ac) can be observed as a small thin cap over the anterior end of the head. The neck region is represented by the constriction between the head and the midpiece (arrow). The proximal and distal centrioles are surrounded by striated cylindrical fibrous sheath. The axoneme (Ax) is outgrowing from the distal centriole. The principal piece consists of 9+2 axoneme. Cross section of centrioles shows the typical array of nine triplets of microtubules. Ac = Acrosome, Ax = Axoneme, H = Head, Mi = Mitochondria, MP = Midpiece, PP = Principal piece, EP = End piece

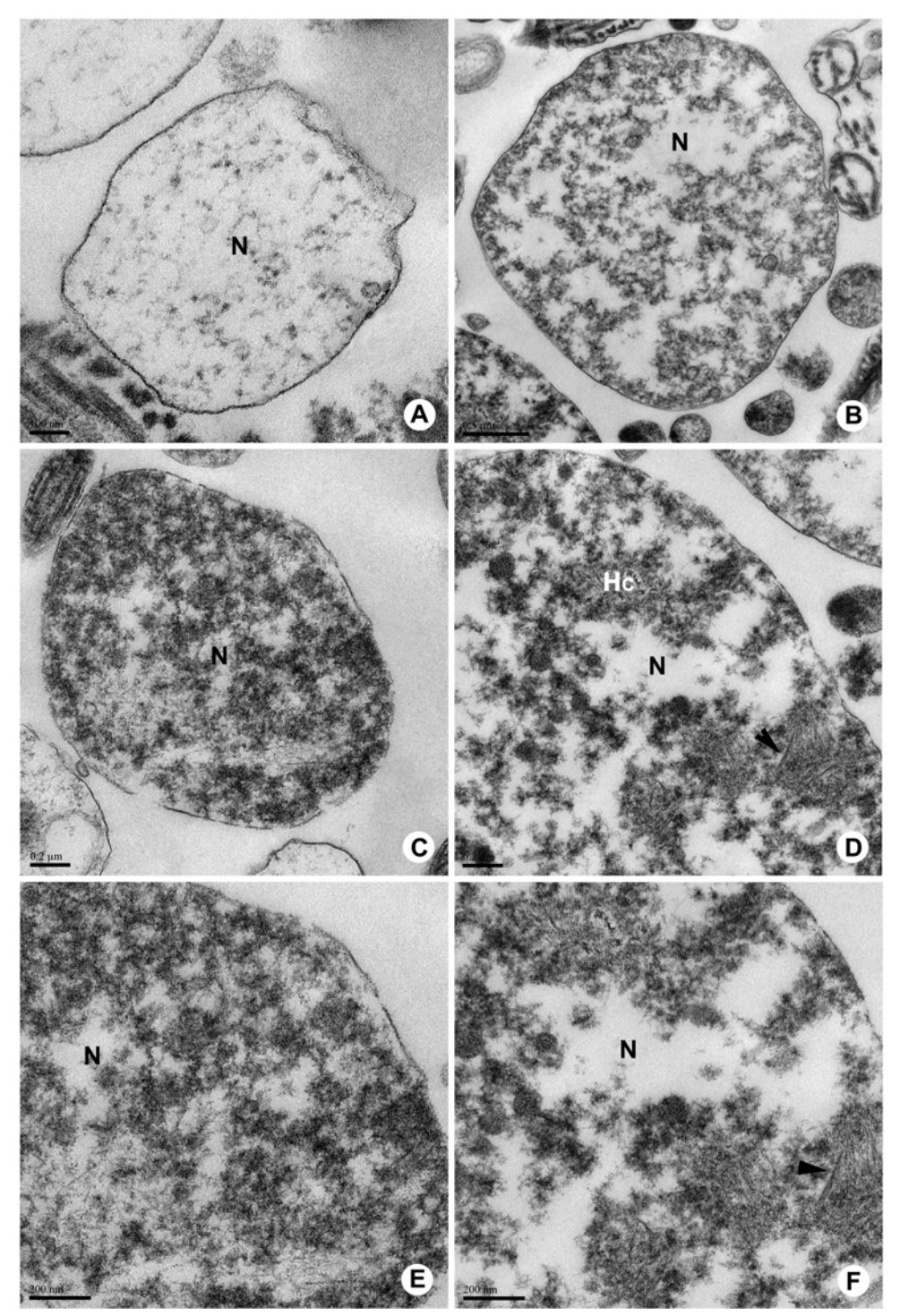


Figure 5 TEM micrographs of longitudinal and cross sections of immature spermatozoa characterized by round to oval nuclei (N) with uncondensed chromatin. The round shaped nucleus shows loosely packed chromatin to form ill-defined dense heterochromatin patches (Hc), while the rest of chromatin are loosely distributed throughout the nucleus. The axes of chromatin condensation appear as single dense lines (arrowhead) are observed. Some nuclei show mostly euchromatin (A). N = Nucleus, Hc = Heterochromatin

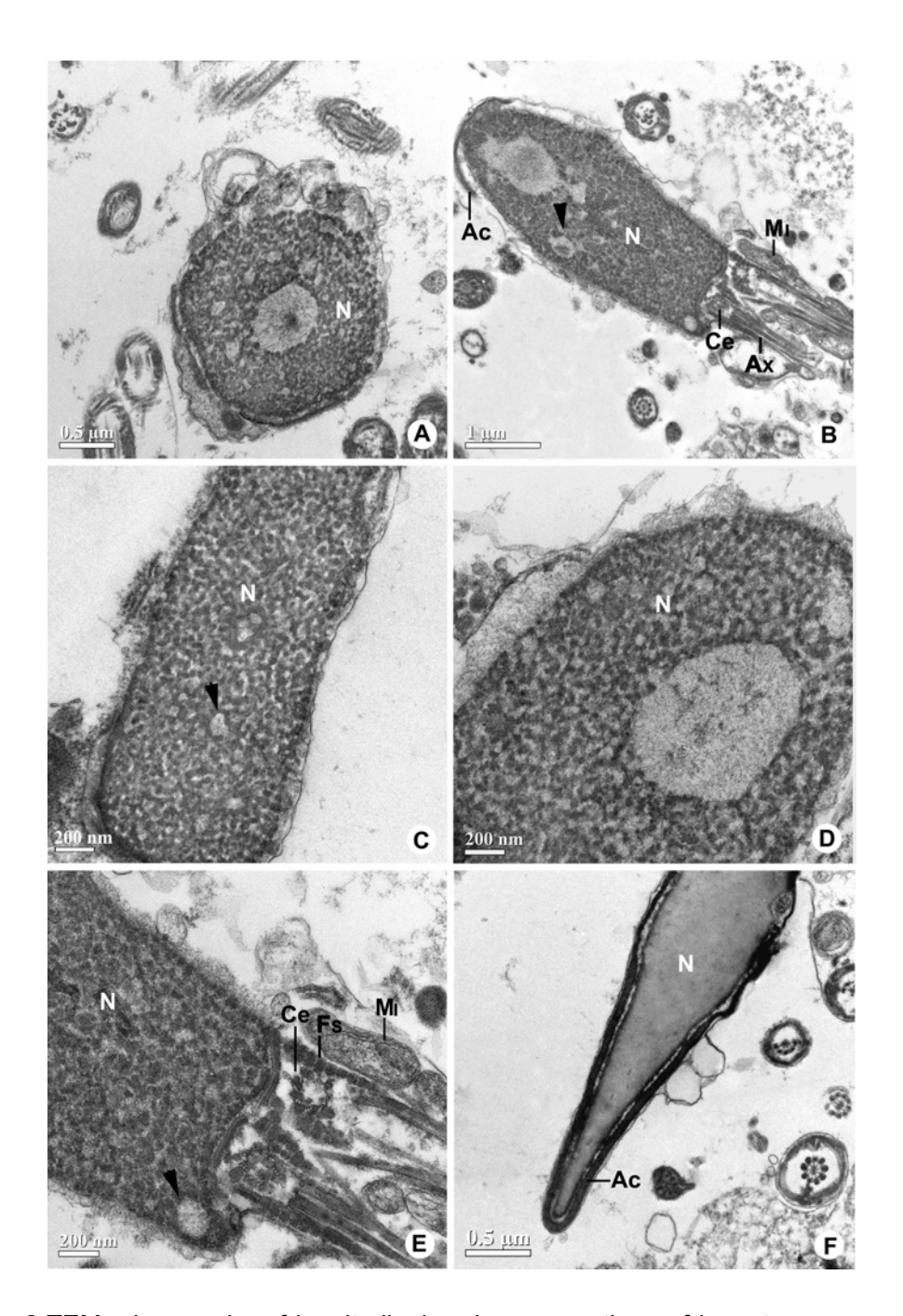


Figure 6 TEM micrographs of longitudinal and cross sections of immature spermatozoa characterized by nuclei with incomplete chromatin condensation (A-E) in comparison to mature spermatozoa with complete chromatin condensation (F). The individual chromatin fibers are closely packed together however small spaces between chromatin fibers are still visible. Some nuclear vacuoles are observed (arrowhead). The centrioles (Ce) are surrounded by striated cylindrical fibrous sheath (FS), start to form the axonemal complexes of the tail. The caudal end of the nucleus contains mitochondria (Mi) and substantial amount of cytoplasm. Ac = Acrosome, Ax = Axoneme, Ce = Centriole, N = Nucleus, FS = Fibrous sheath, Mi = Mitochondria

2. Distribution of Transition Protein and Protamines in Spermatozoa of Infertile Couples as Studied by Immunoelectron Microscopy

Immunogold labeling with anti-protamine1 antibody was found over the nuclei of spermatozoa from infertile couples. The labeling was especially abundant in the area of highly condensed chromatin (Fig. 8B, D, F), with only occasional gold particles observed over the area of incomplete chromatin condensation (Fig. 8A, C, E). The labeling appeared to be directly proportional to its condensation state. There was no labeling in the nuclear vacuoles of the sperm nuclei. The cytoplasm showed only minimal background level of labeling. In control group, only a low background immunogold labeling can be observed (Fig. 7).

Immunogold labeling with anti-protamine 2 antibody revealed the distribution of gold particles over the nuclei of spermatozoa from infertile couples, and their abundance is directly proportional to the state of chromatin condensation. Only a few gold particles were found in the areas of incomplete condensed chromatin (Fig. 10C, D) Interestingly, higher amount of immunogold labeling was observed in the nuclei of spermatozoa from infertile couples with morphologically normal spermatozoa >4% (Fig. 10) in comparison to spermatozoa from infertile couples with morphologically normal spermatozoa <4% (Fig. 11). There was an absence of labeling in the nuclear vacuoles of the sperm nuclei. No labeling was also obtained in the cytoplasm of the spermatozoa. In control group which was incubated in the absence of primary antibody, only background labeling was observed.

When the spermatozoa from infertile couples with morphologically normal spermatozoa >4% were incubated with anti-TP antibody, little to no labeling was observed over the nuclei (Fig. 12). In contrast, the labeling was prominent over the granular and condensed chromatin of spermatozoa from infertile couples with morphologically normal spermatozoa <4% (Fig. 13). Only background level of labeling can be observed in control group.

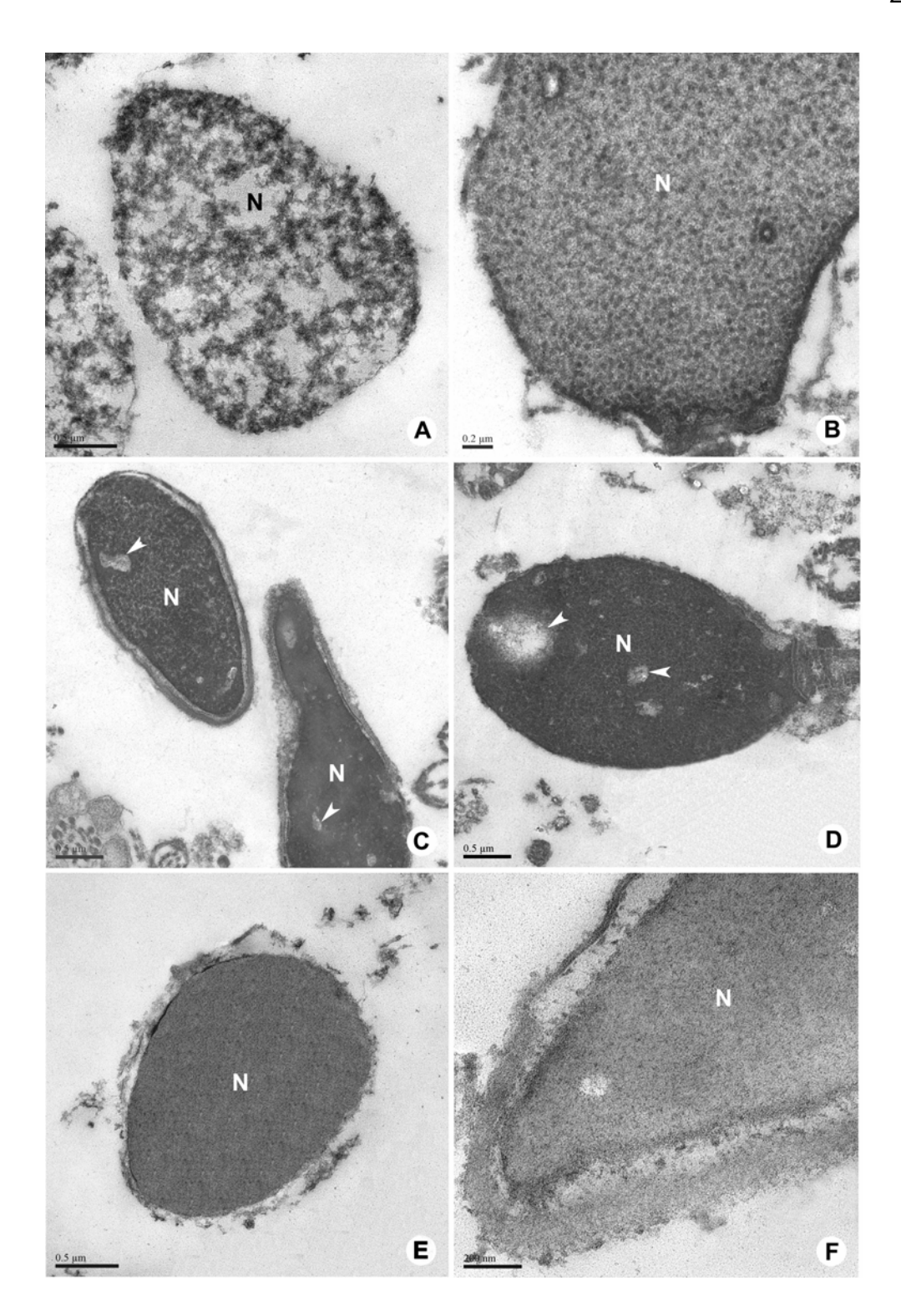


Figure 7 TEM micrographs of spermatozoa from infertile couples incubated in the absence of primary antibody and labeled with immunogold. No gold particle was observed in the nuclei of both incomplete condensed (A-D) and condensed chromatin (E-F). N = Nucleus Arrowhead = Nuclear vacuole